Design of a Thorium Extraction Process from Monazite Sand

A Capstone Report
presented to the faculty of the
School of Engineering and Applied Science
University of Virginia

by

Karl Westendorff

with

Ben Newhouse
Samuel Ong
Peter Sepulveda
Anna Winter

May 8, 2021

On my honor as a University student, I have neither given nor received unauthorized aid on this assignment as defined by the Honor Guidelines for Thesis-Related Assignments.

Karl Westendorff

Technical or Capstone advisor: Eric Anderson, Department of Chemical Engineering

SUMMARY

The looming effects of global climate change mandate the adoption of clean energy sources. Nuclear power plants are carbon-neutral energy producers, but economic and safety concerns inhibit their widespread implementation. Thorium nuclear fuels are an attractive alternative to their currently used uranium counterparts because of their higher natural abundance and safer disposal options. A continuous process to extract thorium from monazite sands and convert it to its oxide at a nuclear fuel grade purity (>92 %) is described with the aim of making safer nuclear fuels more accessible.

The proposed process consists of thorium isolation, thorium purification, and thorium oxide formation blocks. The thorium isolation block digests the monazite sand feed in sulfuric acid and selectively precipitates the desired thorium compounds in ammonium hydroxide. The thorium purification block converts the thorium hydroxide precipitate to its nitrate form, after which an extraction and stripping process with TBP, Kerosene, and water purifies the thorium components to specification. The thorium isolation block converts the purified thorium nitrate to its oxalate salt through precipitation in oxalic acid and combusts the resulting solid in a rotary kiln to form thorium oxide.

The process consumes 300,024 kg of monazite sand per year, produces 30,513 kg of thorium oxide annually, and utilizes 85,061 kWh per year. After a startup cost of $2.7 million, economic analyses indicate the plant is profitable at its designed scale in two years with an annual non-discounted cash flow of $8.2 million.

The proposed process requires significant safety, environmental, and social considerations. Plant safety concerns include mildly radioactive material moving throughout the plant, inhalation dangers associated with processed sands and powder products, and the handling of strong acids and bases. Environmental considerations include the proper disposal of rare earth element waste streams. If constructed, the proposed plant has the potential to significantly impact the nuclear industry and provide a domestic source of carbon-free fuel for the United States.

I. INTRODUCTION

Hydrocarbon fuels such as coal and oil are the primary sources of global energy production due to their low costs and relatively high energy densities. These fuels are combusted to generate heat and produce numerous by-products such as sulfates, heavy metals, methane, and carbon dioxide (Peter, 2018). Their emissions are traditionally vented into the atmosphere and have negatively impacted the environment. Sulfate and heavy metal particulate emissions damage human respiratory systems, poison wildlife, and contribute to the acidification and destruction of natural ecosystems. Methane and carbon dioxide greenhouse gas emissions trap heat within the Earth's atmosphere and contribute to increasing temperatures worldwide; this has resulted in rising sea levels and the extinction of animal species. The increasingly adverse consequences of global warming motivate the development of alternative energy sources that have less detrimental environmental effects (Union of Concerned Scientists, 2017).

Nuclear power functions through the propagation of fission reactions where atomic nuclei are split to release large amounts of energy. Because of this significant energy output, nuclear reactors exist to safely maintain fission processes. There are currently 57 nuclear power plants in operation in the United States which sustain approximately 20% of the country's energy demand (U.S. Energy Information Administration, 2020). The predominant fuel source used in these power plants is uranium. The fission of uranium fuels does not produce any greenhouse gases, but does produce radioactive waste. The used fuel is highly radioactive and must be removed and stored under strict measures to ensure it does not harm the surrounding environment. It is decades before the waste is rendered safe, and storage of these compounds has become a major deterrent for the wide-scale implementation of nuclear energy. Additionally, this nuclear waste can be utilized in nuclear weapons through re-processing, meaning that the storage of this material must be handled with extreme security (Brady, 2019).

Thorium has recently gained attention as an attractive alternative to uranium for nuclear fuel. It is three times more abundant than uranium, making it one of the most abundant nuclear fuels on Earth (World Nuclear Association, 2017). This makes nuclear reactors viable in areas such as India and Brazil where uranium is scarce, as their thorium deposits are able to serve the same function. Additionally, the waste produced by thorium fuels decays at a faster rate, meaning that less storage time is necessary to ensure its proper disposal. The radioactive isotopes present within this waste are also less weaponizable due to their chemical structure, reducing security concerns considerably (Bahri et al., 2015).

This report details a continuous process to extract thorium from monazite sands and convert it to its oxide at a nuclear fuel grade purity (>92 %) with the aim of making safer nuclear fuels more accessible (Salehuddin, 2019). Additionally, monazite sands are present in several countries with developing economies, and the scaled-up thorium extraction process described here provides a pathway towards utilizing this largely untapped resource (Hania & Klaassen, 2012).

II. PREVIOUS WORK

II.A Current REE Extraction Methods

While thorium's use as a nuclear fuel is an emerging topic, rare earth element (REE) extraction is a well documented area of research. REEs commonly appear alongside each other in a variety of naturally occurring ores including monazite, xenotime, laterite, and bastnasite, motivating the development of isolation methods. This review focuses on monazite processing operations because of its high thorium concentration. Three processes are examined to assess how current REE extraction methods motivate this project.

Shaw (1953) describes a batch process where monazite sand is processed and separated into thorium rich, uranium rich, and REE rich streams. The monazite is first leached in 93% sulfuric acid before being sent to several decanting and filtration steps. From there, separation occurs in three precipitation vessels and is neutralized with ammonia. Thorium is precipitated at a pH of 1.05, REEs at 2.3, and uranium at 6.0. The remainder of the stream is considered waste and the process is complete. Shaw provides insight into early iterations of this process which focused on a full separation of the individual elements.

Rodliyah (2015) investigated REE leaching from monazite and briefly described downstream processing steps. Like Shaw (1953), Rodliyah uses sulfuric acid in the leaching step, but suggests a digestion time of 150 minutes at 220°C and recommends a more dilute acid concentration of 33% by volume. Several REEs were successfully extracted from monazite using this method, but the highest extraction efficiency was only 28.41%. Like Shaw (1953), subsequent separations took place in precipitation vessels using acid-base chemistry. Rodliyah (2015) assessed different potential operating conditions to digest monazite sand into an acidic solution and showed the impacts on downstream processes.

Salehuddin et al. (2019) analyzed the economics of thorium extraction from monazite sand, outlined the required unit operations, and detailed their parameters. While the presented process is unique, the chemistry is cited from several other studies. In Salehuddin's batch process, 98% sulfuric acid is used to leach monazite sand at 230°C for four hours. The leached sulfates are then filtered and sent to a precipitation vessel where ammonium hydroxide is used to separate thorium rich solids at a pH of 1.84. Nitric acid is added to produce nitrates which are further separated in a mixer settler extraction system. The remainder of the process uses calcination techniques to obtain a final product of thorium oxide. Salehuddin's study outlined a modern process for the separation of thorium from monazite and serves as a foundation for this thesis.

II.B Current Thorium Oxide Isolation Methods

The thorium oxide isolation process consists of two key components: an oxalate precipitation step and an oxide calcination step. While exact operating parameters vary between studies, their methods' fundamentals remain the same, and both processes are well documented.

A baseline study of the oxalate precipitation step was conducted by White et al. (1980). Operating temperatures of 10 and 70 °C, residence times of 15 and 360 minutes, and agitation methods of mechanical and polytronic functionalities were tested to determine the optimal configuration. Lower temperatures were found to increase the theoretical density by up to 96%, whereas higher temperatures were able to achieve a density of 94%. Residence time and agitation method had little effect on product densities. As such, the study determined that operation conditions of 10 °C, with a residence time of 15 minutes and mechanical agitation were optimal, as it required the least amount of energy and was able to consistently achieve thorium oxide purities of nuclear fuel grade (> 92%).

Wangle et al. (2017) studied how different manufacturing procedures affect thorium oxide quality by manipulating both the oxalate precipitation and calcination steps and aimed to produce oxide products that were able to pack and sinter easily. They determined that the choice of precipitation method and calcination temperature was crucial to obtaining optimal final product morphologies by testing a variety of different procedures. Lab-scale experiments were performed where oxalic acid and thorium nitrate were added dropwise to one another, agitated to precipitate solid material, and calcined at different temperatures (500 to 1750 °C) to isolate the final product. It was found that novel agitation methods, such as ultrasonication, had little effect on the final product, with packing densities remaining high between 98.1 and 98.7% for all techniques. Similarly, higher calcination temperatures were able to maintain the packing density of the oxide products above 98%, with the highest being 98.7%. More importantly, higher temperatures were able to produce pellets with homogeneous microstructures, reducing unpredictability and standardizing the product material. At 700°C, these improvements plateaued, making higher temperatures unnecessary.

Oxalate precipitation and oxide calcination processes have changed very little in the past few years; their optimal conditions are well-established in literature and are cited by reports concerning scaled-up systems such as Salehuddin et al. (2019). In this process, thorium oxalate is precipitated with the addition of 2 M oxalic acid. The solids are fed to a rotary kiln operating at 1000 °C to calcine and produce solid thorium oxide products.

III. DISCUSSION

III.A Overall Design Basis

The proposed process has three sections: thorium isolation, thorium purification, and thorium oxide formation. The monazite sand used within this plant is assumed to have a set concentration of thorium, cerium, lanthanum, and neodymium phosphates, specified in **Table III.A.1-1.** In the thorium isolation block (Block 1), monazite sands are fed into a sulfuric acid leaching reactor where RE phosphates are converted to sulfates. These sulfates are then combined with 13.4 M ammonium hydroxide and thorium hydroxide is selectively precipitated out of solution. In the thorium purification block (Block 2), the thorium hydroxide is converted to thorium nitrate after mixing with nitric acid, and this nitric acid stream is then purified via an extraction and stripping process with TBP/Kerosene and water, respectively. In the thorium oxide formation block (Block 3), the purified thorium nitrate stream is mixed with oxalic acid to form and precipitate thorium oxalate out of solution. The thorium oxalate is then fed to a calcination kiln where it is burned to yield thorium oxide at >92% purity.

The system was designed to produce enough thorium oxide fuel for nuclear power plants to meet the annual energy requirements of Virginia and its surrounding states, based on the historical power consumption of Virginia and North Carolina. This requires a monazite sand feed of 41.67 kg/hr, which is 4% of the world's current monazite supply. The proposed system requires approximately 284 kWh/day of energy to operate. Aside from the feed and product streams, there are six waste streams. From Block 1, there are solid residue streams after both the sulfuric acid leaching reactor and the selective precipitation vessel. From Block 2, there are waste streams out of the extraction vessel and a solid residue stream after the stripping column. Finally, from Block 3, there is a dilute nitric acid waste stream and a flue gas stream from the rotary kiln. The overall process flow diagram (PFD) for this process is detailed in **Figure III.A.1-1**.

Table III.A.1-1. Monazite Sand Composition

Component	% Composition
$Th_3(PO_4)_4$	15.00
$CePO_4$	45.00
$LaPO_4$	25.00
$NdPO_4$	15.00

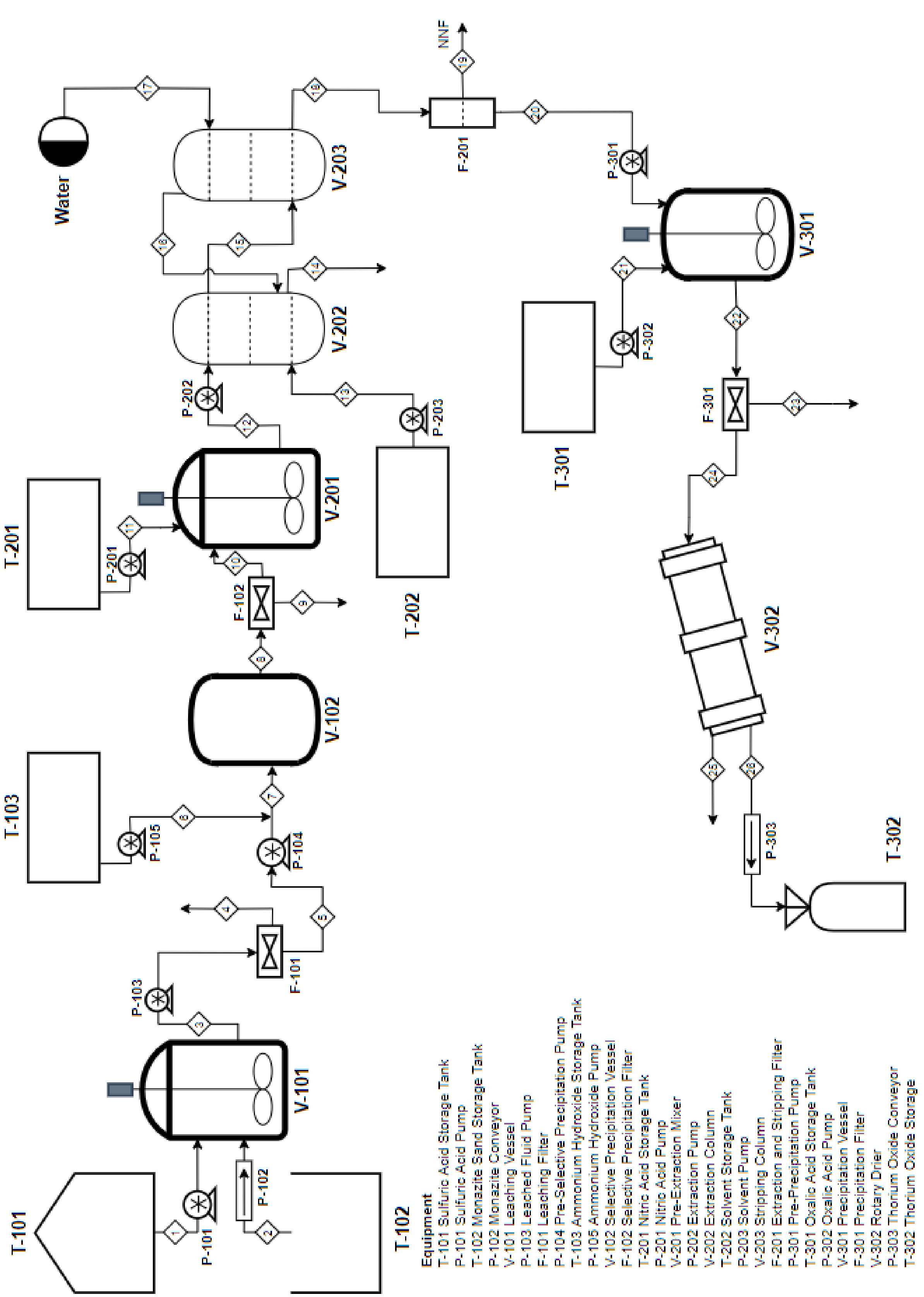

Figure III.A.1-1. Overall PFD of system.

III.B. Block 1: Thorium Isolation

III.B.1 Thorium Isolation Overview

Block 1 focuses on the isolation of thorium from the other rare earth elements in the initial monazite sand feed. This is accomplished in two steps: first by leaching the monazite sand with 98% sulfuric acid, and second by converting the rare earth phosphates into sulfates. These aqueous rare earth sulfates and remaining filtrate are then mixed with 13.4 M ammonium hydroxide and sent to a selective precipitation vessel, where the majority of the thorium and smaller amounts of the other rare earth elements precipitate out as hydroxides. The process flow diagram for Block 1, including auxiliary equipment, is displayed in **Figure III.B.1-1**.

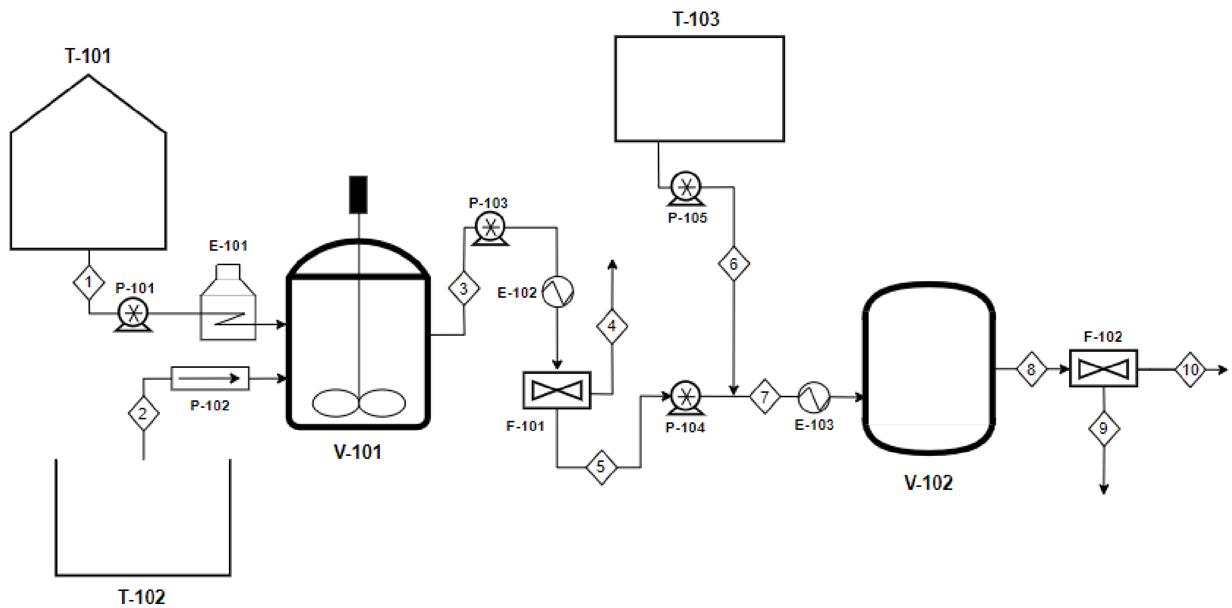

Figure III.B.1-1. Block 1 PFD.

III.B.2 Sulfuric Acid Leaching

Monazite sand is a mixture of REE phosphates of varying compositions, and this solid needs to be converted into an aqueous solution before further processing. Digestion with sulfuric acid dissolves the valuable REE species and leaves a residue which is removed in waste stream 4. **Eqn. III.B.2-1** describes this process explicitly for thorium phosphates in monazite sands and **Eqn. III.B.2-2** describes this process generally for other rare earth (RE) elements, which predominantly include Ce, La, and Nd.

$$Th_3(PO_4)_4(s) + 6H_2SO_4(aq.) \rightarrow 3Th(SO_4)_2(aq.) + 4H_3PO_4(aq.) \qquad \textbf{(Eqn. III.B.2-1)}$$

$$2(RE)PO_4(s) + 3H_2SO_4(aq.) \rightarrow RE_2(SO_4)_3(aq.) + 2H_3PO_4(aq.) \qquad \textbf{(Eqn. III.B.2-2)}$$

To leach the incoming monazite sand, 98% sulfuric acid is fed into a stainless steel reactor at 1 atmosphere and stirred with a 3 blade hydrofoil with 22% solidity ratio impeller, in agreement with the recommendations made by Prof. Michael L. King at the University of Virginia's chemical engineering department. Throughout this report, Prof. King's recommendations are used for impeller types, baffles, and other mixing parameters.

It was assumed that 90% of the incoming monazite is dissolved with a 2 hour residence time, in accordance with the results reported by Demol et al. (2018). The remaining 10% is removed in waste stream 4. All compounds in monazite were assumed to dissolve at the same rate, and the volume of the tank was assumed to be constant throughout the reaction. The viscosity of the system was assumed to be in between that of sulfuric and phosphoric acid. The resulting vessel and impeller parameters are listed in **Table III.B.2-1**, and the mass balances for this unit operation are listed in **Table III.B.2-2**. The geometric proportions used to determine various parameters of the agitation tank are given in **Eqns. III.B.2-(3-6)** where C_{bot} is the bottom impeller clearance, C_{top} is top impeller clearance, T_d is tank diameter, W is impeller width, d_i is impeller diameter, and J is baffle width. These geometric proportions were used for the sulfuric acid leaching reactor vessel and all other vessels with an impeller.

$$C_{bot} = T_d / 3 \qquad \textbf{(Eqn. III.B.2-3)}$$

$$C_{top} = 2T_d / 3 \qquad \textbf{(Eqn. III.B.2-4)}$$

$$W = d_i / 8 \qquad \textbf{(Eqn. III.B.2-5)}$$

$$J = T_d / 12 \qquad \textbf{(Eqn. III.B.2-6)}$$

The thermodynamic quantities for this process were calculated according to the methods and assumptions outlined in **Section XIII.C**. Power requirements and impeller speed were determined to be 4.99 W and 64 RPM, respectively, and these are based on the general empirical correlations presented by King (2019).

Table III.B.2-1. Leaching Reactor Vessel Parameters

Component	**Size (m)**
Fluid Height	0.666
Tank Diameter	0.666
Impeller Diameter	0.300
Impeller Width	0.037
Impeller Height	0.222
Baffle Width	0.055

Table III.B.2-2. Leaching Reactor Flow Analysis

Species	Total Flow Out (kg/hr)	Product Stream Flow (kg/hr)	Waste Stream Flow (kg/hr)
$Th_3(PO_4)_4$ (s)	0.625	0.000	0.625
$CePO_4$ (s)	1.875	0.000	1.875
$LaPO_4$ (s)	1.042	0.000	1.042
$NdPO_4$ (s)	0.625	0.000	0.625
H_2SO_4 (aq.)	58.675	58.675	0.000
H_2O (l)	1.667	1.667	0.000
$Th(SO_4)_2$ (aq.)	6.652	6.652	0.000
$Ce_2(SO_4)_3$ (aq.)	20.401	20.401	0.000
$La_2(SO_4)_3$ (aq.)	11.344	11.344	0.000
$Nd_2(SO_4)_3$ (aq.)	6.780	6.780	0.000
H_3PO_4 (aq.)	15.316	15.316	0.000

III.B.3 Selective Precipitation

Thorium sulfate precipitation is conducted according to parameters provided by Bahri et al. (2018), who dripped 13.4 M NH_4OH solution to precipitate a thorium sulfate feed until a pH of ~1.6 was obtained in a 26°C mixing vessel. This precipitation occurs explicitly by **Eqn. III.B.3-1** for thorium sulfate and by **Eqn. III.B.3-2** for other RE elements.

$$3Th(SO_4)_2(aq.) + 4NH_4OH(aq.) \rightarrow Th(OH)_4(s) + 2(NH_4)_2SO_4(aq.) \qquad \textbf{(Eqn. III.B.3-1)}$$

$$RE_2(SO_4)_3(aq.) + 6NH_4OH(aq.) \rightarrow 2RE(OH)_3(aq.) + 3(NH_4)_2SO_4(aq.) \qquad \textbf{(Eqn. III.B.3-2)}$$

The pH of the incoming solution was found to be -1.7. This factored in the reaction of H_2SO_4, HSO_4^-, and H_3PO_4 with water. The weaker acids were found to have a K_a of negligible magnitude and were not considered. The amount of ammonium hydroxide needed was found using its pK_b of 4.8 and ensuring that there was enough hydroxide ion concentration in the resulting mixture. 13.4 M ammonium hydroxide was used in this process, which roughly equates to a 1:3 ratio of NH_4OH and water. It was calculated that approximately 225 kg/hr of NH_4OH was necessary to reach the desired pH, resulting in a stream flow rate of 900 kg/hr.

Our design is a continuous process, so an impeller would introduce agitation to the vessel and hinder the collection of solid thorium hydroxide precipitate. Mixing was therefore achieved by introducing ammonium hydroxide into the piping with the sulfates under turbulent conditions. To achieve turbulent conditions, the flowing mixture had to have a Reynold's number greater than 2300. The viscosity and density of the mixture was calculated through interpolation between the ammonium hydroxide and the sulfate solutions, and the dimensions of the pipe were manipulated to achieve turbulent flow. It was determined that the pipe has a maximum diameter of 1.98 inches and a minimum length of 20 inches. After complete mixing, the stream is deposited into V-102 where the solids would settle. The exact parameters of the mixing pipe and reactor vessel are given in **Table III.B.3-1** below.

Table III.B.3-1. Selective Precipitation Reactor Vessel and Mixing Pipe Parameters

Component	Size (m)
Tank Height	3.000
Tank Diameter	1.000
Pipe Diameter	0.050
Pipe Length	0.500
Reynolds Number	2834*

*dimensionless

In addition to the reactions concerning the sulfates, it was assumed that the ammonium hydroxide would completely neutralize the remaining sulfuric acid, forming water, ammonium sulfate, and excess heat. Due to the instability of ammonium phosphate, neutralization did not occur between the ammonium hydroxide and the phosphoric acid. The total heat generated in the reactions was calculated to be -700,000 kJ/hr, so to maintain isothermal operating conditions of 35ºC , a cooling jacket surrounding the mixing pipe was added. This jacket has a cooling water flow rate of 8400 kg/hr at a temperature of 30 ºC, where the ΔT is 20 ºC. The thermodynamics concerning the heat of reactions of the rare earth metals and thorium were assumed to be upper bound by the substitution of equivalent yttrium compounds. The total heat of reaction for conversion of the rare earth sulfates to hydroxides were found to be -300,000 kJ/hr. The remaining -400,000 kJ/hr were derived primarily from the neutralization reaction that occurred as a result of the acid-base chemistries within the mixture.

The outlet flows of the selective precipitation are shown in **Table III.B.3-2** below. Note that the hydroxide species are aqueous in the waste stream and solid in the product stream. The separation of thorium and rare earth hydroxides are taken from Bahri et al. (2018), who performed a similar process. 97.7% of the thorium hydroxide is precipitated out into a solid stream alongside 1.61 - 3.08 % of the rare earth hydroxides depending on their element. The total volume of the mixture is approximately 1 m^3 per hour. Using a length to diameter ratio of 3 and a desired 50% capacity, the volume of the tank was set to be 2 m^3, the diameter was calculated to be 0.95 m, and the length then found to be 2.85 m. The vessel is constructed out of stainless steel with an operating pressure of 1 atmosphere. These calculations were made with the expectation of a 60 minute residence time and a negligible volume change during mixing.

Minimal vapor is expected to be generated from this process, but the tank is expected to operate at half-capacity normally to reduce the possibility of overfilling and pressure build-up.

Table III.B.3-2. Selective Precipitation Outlet Flow Analysis

Species	Total Flow Out (kg/hr)	Product Stream Flow (kg/hr)	Waste Stream Flow (kg/hr)
H_3PO_4 (aq.)	15.32	0.00	15.32
NH_4OH (aq.)	166.60	0.00	166.60
$Th(OH)_4$ (s)*	4.71	4.60	0.11
$Ce(OH)_3$ (aq.)*	13.72	0.38	13.34
$La(OH)_3$ (aq.)*	7.61	0.16	7.45
$Nd(OH)_3$ (aq.)*	4.59	0.14	4.45
$(NH_4)_2(SO_4)$ (aq.)	110.00	0.00	110.00
H_3PO_4 (aq.)	696.60	0.00	696.60

*all hydroxides are solid in the product stream flow and aqueous in the waste stream flow.

III.C Block 2: Thorium Purification

III.C.1 Thorium Purification Overview

Block 2 focuses on the purification of the thorium that is being precipitated out of the selective precipitation vessel. This is accomplished by first converting the thorium hydroxide to a nitrate using nitric acid in a jacketed agitated reactor. These aqueous nitrates are then introduced to the top of an extraction column, where they are introduced to a 30/70 mass % TBP/kerosene organic phase. The organic phase is then introduced into the bottom of the stripping column where it is introduced to water. The resulting aqueous phase, containing the majority of the $Th(NO_3)_4$, is transferred to Block 3. The process flow diagram for Block 2, including auxiliary equipment, is displayed in **Figure III.C.1-1**. Note that in the figure, one depicted disk and donut configuration is representative of two necessary disk and donuts for the actual design.

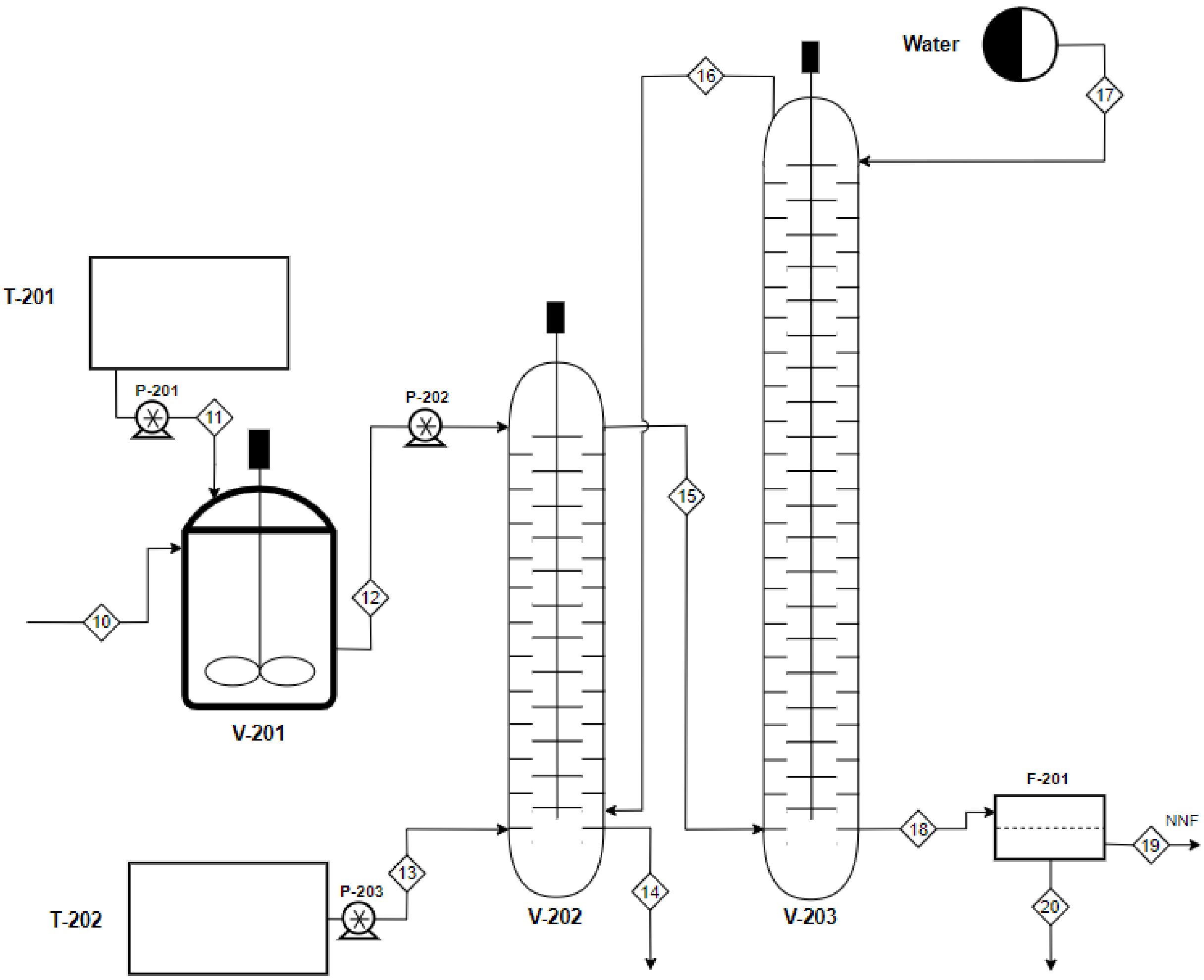

Figure III.C.1-1. Block 2 PFD. Each stage drawn in the extraction and stipping columns represents two designed stages.

III.C.2 Conversion to Nitrates

After thorium is selectively precipitated, it is then converted to its nitrate form to prepare it for further purification. This occurs in tank V-201 according to **Eqn. III.C.2-1**. The stainless steel vessel operates at 50°C and 1 atm to replicate the conditions used by Salehuddin et al. (2019).

$$Th(OH)_4(s) + 4HNO_3(aq.) \rightarrow Th(NO_3)_4(aq.) + 4H_2O(l) \qquad \textbf{(Eqn. III.C.2-1)}$$

Due to the multiple phases present, V-201 employs a 6 blade Rushton turbine whose parameters are described in **Table III.C.2-1**. The geometric proportions used to determine various parameters of the agitation tank were given in **Eqns. III.B.2-(3-6)**. The impeller operates at 239 rpm and requires 0.41 W to operate. V-201 has a residence time of 1 hour, in agreement with the experiments conducted by Moore et al. (1957). The thermodynamic quantities for this process were calculated according to the methods and assumptions outlined in **Section XIII.C**.

Table III.C.2-1. Nitration Reactor Vessel Parameters

Component	Size (m)
Tank Height	0.364
Tank Diameter	0.364
Impeller Diameter	0.182
Impeller Width	0.030
Impeller Height	0.036
Baffle Width	0.030

Mass balances for thorium nitration are described in **Table III.C.2-2**. It was assumed that all incoming hydroxide species were converted to nitrates due to the high excess of nitric acid employed.

Table III.C.2-2. Nitration Outlet Flow Analysis

Species	Total Flow In (kg/hr)	Total Flow Out (kg/hr)
$Th(OH)_4$ (s)	4.60	0.00
$Ce(OH)_3$ (s)	0.38	0.00
$La(OH)_3$ (s)	0.16	0.00
$Nd(OH)_3$ (s)	0.14	0.00
HNO_3 (aq.)	27.81	23.26
H_2O (l)	11.92	13.21
$Th(NO_3)_4$	0.00	7.35
$Ce(NO_3)_4$	0.00	0.66
$Le(NO_3)_3$	0.00	0.27
$Nd(NO_3)_3$	0.00	0.24

III.C.3 Extraction and Stripping

After being converted to nitrates, thorium is then able to undergo an extraction and stripping process to further purify it from other REEs. Extraction parameters for this process are adopted from Bahri et al. (2018) who converted thorium hydroxides to thorium nitrate before extraction by mixing the thorium sulfate stream with 70 mass % nitric acid (**Eqn. III.C.2-1**).

Thorium nitrate in the aqueous phase is then extracted to a 30/70 mass % TBP/kerosene organic phase to further purify thorium components, after which it is stripped with distilled water to return thorium nitrate to an exiting aqueous stream.

$$Th(NO_3)_4(aq.) + TBP(org.) \rightarrow Th(NO_3)_4\bullet TBP(org.) \qquad \textbf{(Eqn. III.C.3-1)}$$

$$Th(NO_3)_4\bullet TBP(org.) + H_2O(l) \rightarrow Th(NO_3)_4(aq.) + TBP\bullet H_2O(org.) \qquad \textbf{(Eqn. III.C.3-2)}$$

Both the stripping and extraction columns utilize a disk-and-donut type of impeller system which operates at 60 rpm. Each column was designed such that the residence time per stage was the same as recorded by Burkart et al. in 1952, and this paired with the number of required theoretical stages from Morello and Poffenberger determined the height and diameter of the final column design (1950). Extraction and stripping column parameters are listed in **Table III.C.3-1** and **Table III.C.3-2**, respectively. Power requirements are based on the general empirical correlations presented by King (2019).

Table III.C.3-2. Extraction Column Parameters

Component	Specifications
Column Height (m)	2.40
Column Diameter (m)	0.74
Tray Spacing (m)	0.18
Number of Trays	24.00
Theoretical Stages	3.00
Volume of Column (m^3)	1.03
Power (W)	114.04
Residence Time (hr)	0.95

Table III.C.3-2. Stripping Column Parameters

Component	Specifications
Column Height (m)	4.00
Column Diameter (m)	0.71
Tray Spacing (m)	0.1
Number of Trays	40.00
Theoretical Stages	5.00
Volume of Column (m^3)	1.57
Power (W)	190.07
Residence Time (hr)	1.58

Heats of reaction for the extraction column were used from Shaeri et al. (2015). For the stripping column, the heat of solvation for TBP and Hess' law was employed to determine the heat of reaction. Mass balances on the extraction and stripping columns are listed in **Table III.C.3-3** and **Table III.C.3-4**. The recycle stream going from the stripping vessel to the extraction was based on the research conducted by Whatley in 1953. The quality of the separation was based on prior assumptions to simplify the mass balance and the empirical results observed by Alreqi et al. (2017) to obtain a 92% purity.

Table III.C.3-3. Extraction Column Mass Balance

Species	Feed Flow (kg/hr)	Solvent Feed (kg/hr)	Recycle Feed (kg/hr)	Aqueous Waste (kg/hr)	Organic Product (kg/hr)
HNO_3 (aq.)	23.27	0.00	0.00	23.27	0.00
H_2O (l)	13.22	0.00	0.00	13.22	0.00
$Th(NO_3)_4$ (aq.)	7.35	0.00	0.00	0.22	7.13
$Ce(NO_3)_3$ (aq.)	0.66	0.00	0.00	0.26	0.39
$La(NO_3)_3$ (aq.)	0.27	0.00	0.00	0.15	0.12
$Nd(NO_3)_3$ (aq.)	0.24	0.00	0.00	0.13	0.11
TBP (org.)	0.00	50.00	250.02	50.0	250.02
Kerosene (org.)	0.00	116.68	583.38	116.68	583.38

Table III.C.3-4. Stripping Column Flow Analysis

Species	Feed Flow (kg/hr)	Aqueous Feed (kg/hr)	Recycle Out (kg/hr)	Aqueous Product (kg/hr)
H_2O (l)	0.00	166.68	0.00	166.68
$Th(NO_3)_4$ (aq.)	7.13	0.00	0.00	7.13
$Ce(NO_3)_3$ (aq.)	0.39	0.00	0.00	0.39
$La(NO_3)_3$ (aq.)	0.12	0.00	0.00	0.12
$Nd(NO_3)_3$ (aq.)	0.11	0.00	0.00	0.11
TBP (org.)	250.02	0.00	250.02	0.00
Kerosene (org.)	583.38	0.00	583.38	0.00

III.D Block 3: Thorium Oxide Formation

III.D.1 Thorium Oxide Formation Overview

Block 3 focuses on the formation of thorium oxide from the aqueous thorium nitrate produced by Block 2. This is accomplished by first introducing the aqueous phase from the stripping column to a precipitation vessel, and adding oxalic acid into the agitated precipitation vessel. This causes the precipitation of thorium oxalate, which is then separated from the liquid and moved to a rotary calcination kiln. The thorium oxalate is then calcined at 900°C to form thorium oxide. The process flow diagram for Block 3, including auxiliary equipment, is displayed in **Figure III.D.1-1**.

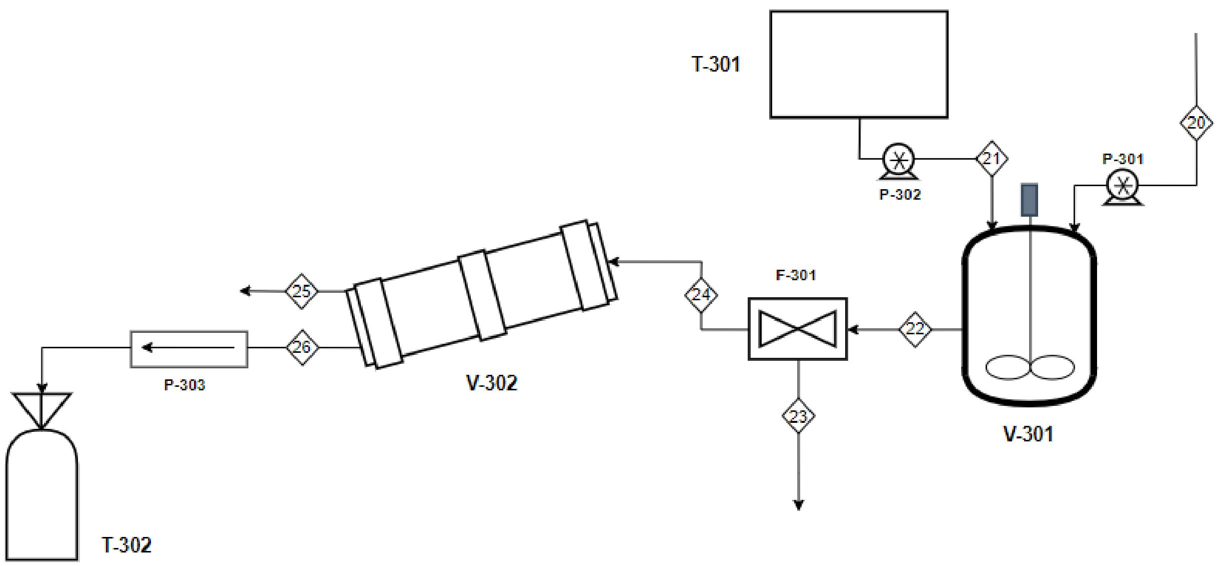

Figure III.D.1-1. Block 3 PFD.

III.D.2 Oxalate Formation and Precipitation

The precipitation of oxalate compounds followed a procedure similar to Wangle et al. (2017) and occurred in a vessel with a 4:3 M ratio of thorium nitrate to oxalic acid, in accordance with **Eqn III.D.2-1.**

$$Th(NO_3)_4(aq.) + 2C_2H_2O_4(org.) \rightarrow Th(C_2O_4)_2 \bullet 4H_2O(s) + 4HNO_3(aq.) \qquad \textbf{(Eqn. III.D.2-1)}$$

Calcination of thorium oxalate occurs in heating cycles as described by Wangle et al. (2017). Initially, furnace temperatures are raised to 350°C and held for 12 hours to prevent melting of the ThO_2 product. The furnace temperature is subsequently raised to 700°C and held for 4 hours to maximize the shrinkage rate of thorium oxalate while preventing end-capping of the resulting ThO_2 powder.

In Wangle et al. (2017), a batch process was employed where oxalic acid was added dropwise into a thorium nitrate solution. This process occurred at 10° C and agitated for 15 minutes for complete mixing. Our process is designed continuously, and modifies this process to account for this. Dropwise addition of oxalic acid is not viable due to the sheer volume of the process, so it is added at a flow rate of 3.32 kg/hr. This combines with the nitrate stream flowing in at 177.5 kg/hr in the mixing vessel, whose composition is defined in **Table III.C.3-4**. To allow for ample time for mixing, the residence time of this mixing vessel was set at 1 hour. Stainless steel is used to construct this vessel and all of its relevant components due to its high corrosion resistance and durability. Additionally, a 6-blade Rushton turbine impeller is used to maintain solid suspension within the tank. A more complete description of the dimensions of the components within the mixing vessel are given in **Table III.D.2-1**. The geometric proportions used to determine various parameters of the agitation tank were given in **Eqns. III.B.2-(3-6)**. After complete mixing, the stream is fed into a filter where the solids and liquids are separated.

Table III.D.2-1. Oxalate Precipitation Vessel Parameters

Component	Size (m)
Fluid Height	0.61
Tank Diameter	0.61
Impeller Diameter	0.43
Impeller Width	0.05
Impeller Height	0.20
Baffle Width	0.05

The thermodynamic quantities for this process were calculated according to the methods outlined in **Section XIII.C**. Thermochemical data for the various thorium and rare earth compounds were used to determine the theoretical heat of reaction. The energy released by this process was approximately 14,400 kJ/hr, with the primary source of heat originating from the thorium reaction. To maintain optimal kinetics, the vessel was designed to operate isothermally at 10° C. To achieve this, the incoming nitrate stream needs to be cooled from 40° C to 10° C. This stream was assumed to have the thermodynamic properties of water due to its composition being 98.6% water, so 22,700 kJ/hr of heat must be stripped from this stream. Cooling water is used to accomplish this task; approximately 361.5 kg/hr of refrigerated water flowing in at 5° C is necessary to do this and is heated to 20° C. A compressor is utilized to achieve this temperature.

The outlet flows of the oxalate precipitation step are shown in **Table III.D.2-2** below. Two streams are produced from this process; a solid product stream and a liquid waste stream. The product stream is composed primarily of thorium and rare earth oxalates, as well as their associated hydrates. The waste stream consists of unreacted oxalic acid, nitric acid produced as a by-product from the reactions, and a majority of the water from the stripping step. These two outlet streams are then separated through a filter, denoted as F-301, where the solid stream is then fed to the calcination step and the liquid stream is removed from the plant as waste.

Table III.D.2-2. Oxalate Precipitation Flow Analysis

Species	Outlet Flow (kg/hr)	Product Out (kg/hr)	Waste Out (kg/hr)
$C_2H_2O_4$ (aq.)	0.13	0.00	0.13
$Th(C_2O_4)_2$ (s.)	6.06	6.06	0.00
$Ce_2(C_2O_4)_3$ (s.)	0.33	0.33	0.00
$La_2(C_2O_4)_3$ (s.)	0.10	0.10	0.00
$Nd_2(C_2O_4)_3$ (s.)	0.09	0.09	0.00
HNO_3 (aq.)	4.11	0.00	4.11
$H_2O(l)$	169.69	1.42	168.27

III.D.3 Calcination

The final step in the process involves the conversion of thorium oxalate into the thorium oxide nuclear fuel through a calcination reaction. In **Eqn III.D.3-1** seen below, hydrated thorium oxalate decomposes into thorium oxide and combustion gases under high heat.

$$Th(C_2O_4)_2 \bullet 4H_2O(s) \rightarrow ThO_2(s) + 2CO_2(g) + 2CO(g) + 4H_2O(g) \qquad \textbf{(Eqn. III.D.3-1)}$$

For this continuous process, a rotary kiln is operated at atmospheric pressure and 900°C which are based off of prior research (Balakrishna et al., 1988). A residence time of 3 hours is used to ensure full conversion of the hydrated oxalates into oxides and requires a heat duty of 6642.3 kJ/hr to maintain adiabatic operation (Wangle, 2020). The volume of the incoming flow is 0.005 m^3. To facilitate this incoming flow, the kiln has a volume of 18.1 m^3, resulting in a filling degree of 13% (which describes the amount of space within the kiln taken up by solid material). Additionally, the kiln is tilted at a 5° angle so that the process moves as intended. The amount of heat necessary to start up the kiln is approximately 19,000 kJ. Waste gases are processed as necessary and the product stream is 92.67% solid thorium oxide. This purity is high enough for nuclear fuel and is a saleable product. The exact mass balance for this process is given in **Table III.D.3-2** below.

Table III.D.3-1. Rotary Kiln Parameters

Component	Size (m)
Kiln Length (m)	34.94
Kiln Diameter (m)	0.813
Kiln Speed (rpm)	0.5
Filling Degree (%)	13
Residence Time (hr)	3

Table III.D.3-2 Calcination Mass Balance

Species	Flow In (kg/hr)	Product Flow Out (kg/hr)	Waste Gas Flow Out (kg/hr)
$Th(C_2O_4)_2$ (s)	6.06	0.00	0.00
$Ce_2(C_2O_4)_3$ (s)	0.33	0.00	0.00
$La_2(C_2O_4)_3$ (s)	0.10	0.00	0.00
$Nd_2(C_2O_4)_3$ (s)	0.09	0.00	0.00
H_2O (s)	1.42	0.00	1.41
CO (g)	0.00	0.00	0.91
CO_2 (g)	0.00	0.00	1.43
ThO_2 (s)	0.00	3.92	0.00
Ce_2O_3 (s)	0.00	0.20	0.00
La_2O_3 (s)	0.00	0.06	0.00
Nd_2O_3 (s)	0.00	0.05	0.00

The amount of carbon monoxide leaving in the waste gas stream is significant and requires processing before the waste gas can be emitted. There are a few options available for converting the carbon monoxide but a catalytic converter is sufficient for a process of this scale. The total waste gas flow rate is 3.75 kg/hr which is well within the limits of what a typical passenger vehicle catalytic converter can effectively process. Gas leaving the rotary kiln is hot enough for the catalytic converter to operate at its designed efficiency (Tsinoglou et al., 2004).

III.E Auxiliary Equipment

III.E.1 Heat Exchangers

The design specifications for the leaching reactor require the sulfuric acid feed to be heated to 230ºC prior to entering the vessel in a fired heater, E-101. Many of the assumptions regarding efficiencies, heat transfer coefficients, and cooling water temperatures were obtained from Peters et al. (2002). Design parameters for certain aspects of auxiliary equipment were based on information from Turton et al. (2018). For a flow rate of 83.33 kg/hr, the total heat required to raise the temperature of the acid from 25 to 230ºC was calculated to be 24,516.07 kJ/hr. Using a furnace efficiency of 0.7, 9728.60 W are required to heat the acid. Assuming a radiation and convective rate of heat transfer inside the furnace to be 38,000 and 12,000 W/m^2, respectively, the required heat transfer area for the acid stream was found to be 0.19 m^2. Using a heat of combustion of 49 MJ/kg and a density of 0.68 kg/m^3, it was calculated that 1.05 m^3 of natural gas is needed per hour to achieve the necessary heat requirement. Because sulfuric acid at 98% is actually not corrosive enough to require more resilient materials, the piping can be schedule 40 carbon steel. After leaving the heater, the piping is covered in 85% magnesia to prevent heat losses to the atmosphere and for safety purposes.

The stream exiting the leaching reactor needs to be cooled from 230 to 35ºC prior to filtration and mixing with the ammonium hydroxide, and this change occurs in E-102. Yttrium species heat capacities were used in place of thorium and the other rare earths due to lack of data, and the heat capacity equations were found by running computational calculations on the species at different temperatures and then regressing, of which more information can be seen in **Appendix XII.D**. Using the heat capacity equations for phosphoric acid, yttrium sulfate, and yttrium phosphate in **Eqns. III.E.1-1**, **III.E.1-2**, and **III.E.1-3**, respectively, the heat removal requirement, Q, was calculated to be 27,889.19 kJ/hr (NIST, 1998).

$$C_p(T) = 55.20955 + 301.3204T - 0.095194T^2 + 0.04231T^3 + \frac{0.000512}{T^2} \quad \textbf{(Eqn. III.E.1-1)}$$

$$C_v(T) = -6.05471 \times 10^{-4}T^2 + 8.10281T + 70.5982 \quad \textbf{(Eqn. III.E.1-2)}$$

$$C_v(T) = -2.19428 \times 10^{-4}T^2 + 0.28202T - 16.2945 \quad \textbf{(Eqn. III.E.1-3)}$$

For a cooling water stream that enters at 30ºC and exits at 50ºC, a flow rate 333.28 kg/hr is required. Due to the lack of heat transfer data on rare earth phosphate species, the overall convective heat transfer coefficient, U_0, was assumed to be 850 W/m^{2}K for water to liquid transfer according to Peters et al. (2002). The fouling factor, R_f, for cooling water was found from Turton et al. (2018) to be 1.76×10^{-4} m^{2}K/W, and then the new overall heat transfer coefficient was calculated with **Eqn. III.E.1-4**.

$$\frac{1}{U} = \frac{1}{U_0} + R_f \quad \textbf{(Eqn. III.E.1-4)}$$

The log mean temperature difference (LMTD), ΔT_{lm}, was calculated using **Eqn. III.E.1-5**, where ΔT_1 is the difference between the leached stream input temperature and the cooling water outlet temperature, and ΔT_2 is the opposite.

$$\Delta T_{lm} = \frac{\Delta T_2 - \Delta T_1}{ln\left(\frac{\Delta T_2}{\Delta T_1}\right)} \quad \textbf{(Eqn. III.E.1-5)}$$

The LMTD correction factor, F, was found by using **Eqns. III.E.1-6** and **III.E.1-7** and assuming a shell and tube heat exchanger with 1 shell pass and at least 2 tube passes.

$$S = \frac{T_{tube,out} - T_{tube,in}}{T_{shell,in} - T_{tube,in}} \quad \textbf{(Eqn. III.E.1-6)}$$

$$R = \frac{T_{shell,in} - T_{shell,out}}{T_{tube,out} - T_{tube,in}} \quad \textbf{(Eqn. III.E.1-7)}$$

Calculating a ΔT_{lm} of 48.83 K and a correction factor of 0.5, **Eqn. III.E.1-8** was then used to determine the required heat transfer area, A_0, which was found to be 1.54 m^2.

$$Q = UA_0F\Delta T_{lm} \quad \textbf{(Eqn. III.E.1-8)}$$

While the leached solution is more viscous than the cooling water, because the sulfuric acid is no longer highly concentrated the stream is highly corrosive, to improve reliability and to ease maintenance, the leached solution was designed to flow through the tube side. Additionally, since the leached stream never comes into contact with the shell side, the capital cost is lower as only the tube side needs to be made of stainless steel. The shell and tube heat exchanger operates in countercurrent, with 6 tubes and 2 tube passes on a 0.45 inch square pitch. The tubes are schedule 40 pipes with a ¼ inch nominal diameter, and the shell is schedule 80 pipe with a 2 inch nominal diameter. The heat exchanger is 5 feet in length, with baffles with a 20% cut every foot.

Table III.E.1-1 Leaching Cool-Down Heat Exchanger Specifications

Operating Condition	Tube Side	Shell Side
Inlet Temperature (ºC)	230	30
Outlet Temperature (ºC)	35	50
Flow Rate (L/hr)	57.46	333.28
Material of Construction	Stainless Steel	Carbon Steel

The mixing of the ammonium hydroxide with the filtered leached stream is to be performed inside of a pipe instead of a reaction vessel, and the pipe must operate isothermally and under turbulent conditions, or where the Reynolds number is larger than 2300. E-103, a double-pipe heat exchanger is to be used as large amounts of heat are being produced in the chemical reaction and with precipitate and acid present in the tubes, maintenance would be simpler under this design, though as heat transfer area is smaller compared to another design a larger amount of cooling water is needed.

For a cooling water inlet and outlet temperature of 30 and 50ºC, respectively, a flow rate 8,377.46 kg/hr is required to absorb heat generated by the reaction. The inner pipe, containing the chemical reaction, is a stainless steel schedule 40 pipe with a 1-½ inch nominal diameter. The Reynolds number for the stream was calculated to be 2834.28, well above the required value of 2300. To achieve sufficient mixing, the pipe is to be at 0.5 m long, just over 10 times the inner diameter of the pipe. The cooling jacket is a carbon steel schedule 40 pipe with a 4 inch nominal diameter, with the water flowing through the jacket at 0.36 m/s.

The thorium oxide product that leaves the calcination kiln is at 900ºC and is cooled down to atmospheric temperature via simple convection with the atmosphere on a conveyor. Using the **Eqn. III.E.1-9** for ThO_2 heat capacity, 990.58 kJ/hr of heat needs to be removed from the product to bring it down to around 25ºC (Victor and Douglas, 1961).

$$C_p(T) = 17.057 + 18.06 \times 10^{-4}T - \frac{2.5166\times10^5}{T^2} \qquad \textbf{(Eqn. III.E.1-9)}$$

Because the final product is a powder, using a fan or other form of air cooler could disperse radioactive, toxic particles into the air, also resulting in a loss of product. Additionally, there is no necessity to rapidly cool down the product once it exits the kiln, so allowing it to simply cool down via convective heat transfer with the atmosphere was deemed to be an effective solution, and no fan or heat exchanging device was needed.

III.E.2 Feed and Product Storage Vessels

Both feed deliveries and product shipments are scheduled to take place every week, however, in order to compensate for potential variance, the feed and product storage units were designed to be able to hold 2 weeks worth of material. At the time of delivery, each tank holds roughly 4 to 5 days of material. This ensures that the tanks are not likely to ever be truly empty or at full capacity. **Table III.E.2-1** contains the necessary volumes, material of construction, and type of storage for these vessels.

Table III.E.2-1. Storage Tank Data

Vessel	Stored Content	Volume (m^3)	Material of Construction	Tank Type
T-101	Sulfuric Acid	15.22	Carbon Steel (Moon Fabrication Corporation, 2018)	Enclosed Tank
T-102	Monazite Sand	2.69	Concrete	Enclosed Silo
T-103	Ammonium Hydroxide	311.75	Carbon Steel (Tanner Industries, Inc., 2016)	Floating Roof Tank

T-201	Nitric Acid	8.78	Stainless Steel (GI Tanks, 2018)	Enclosed Tank
T-202	Kerosene/TBP	58.83	Carbon Steel	Floating Roof Tank
T-301	Oxalic Acid	0.68	Carbon Steel (Wiersma et al., 2011)	Enclosed Tank
T-302	Thorium Oxide	0.13	Woven polypropylene (ULINE, 2020)	Bag

III.E.3 Intermediate Storage Vessels

Intermediate storage was designed in case production needed to halt for a specific area of the process without stopping other parts of the process. Intermediate storage should be placed after F-102, the selective precipitate filter, and after F-201, the extraction and stripping filter. These intermediate storage tanks should be able to hold 8 hours of material coming out of both of these filters. **Table III.E.3-1** contains the necessary volumes, material of construction, and type of storage for these two vessels. As these are auxiliary tanks not necessary for normal production, that have not been included in the PFD.

Table III.E.3-1. Intermediate Storage Tank Data

Vessel	Stored Content	Volume (m^3)	Material of Construction	Tank Type
T-104	Block 1 Intermediate Storage	0.25	Carbon Steel	Enclosed Silo
T-203	Block 2 Intermediate Storage	1.40	Carbon Steel	Enclosed Tank

III.E.4 Pumps

The pumps used throughout the process are rotary due to the low flow rates of the streams, with the exception of the two vacuum pumps. Using the guidelines from Peters et al. (2002), and Anderson (2021), which details 0.5 atm for losses in pipes, 0.5 atm for heat exchangers, and ⅓ the total frictional loss if a control valve is present), the differential pressures and hydraulic power values were calculated for each of the pumps, shown in **Table III.E.4-1**. The pump for the stream leaving the leaching reactor is 230°C, so this pump needs to be able to handle these conditions. For acidic streams, the pumps need to be made of corrosion resistant material. Every pump has a spare so that the process can continue in the event of a failure.

Table III.E.4-1. Pump Properties and Specifications

Pump	Stream	Q (L/min)	ρ (kg/m^3)	Δh (m)	ΔP_{head} (Pa)	$\Delta P_{frictional}$ (Pa)	ΔP_{total} (Pa)	P_{hyd} (W)	$P_{operating}$ (W)
P-101	[1] H_2SO_4 Feed	0.755	1823.2	0.67	11900	135100	147000	1.849	2.935

P-103	[3] Leaching fluid	0.967	2155.1	0.00	0	135100	135100	2.177	3.455
P-104	[5] Filtered leaching fluid	0.953	2112.5	0.95	19667	67550	87217	1.386	2.200
P-105	[6] NH_4OH Feed	15.464	970.0	0.95	9031	67550	76581	19.737	31.329
P-201	[11] HNO_3 Feed	0.436	1506.0	0.36	5372	67550	72922	0.530	0.841
P-202	[12] HNO_3 CSTR exit	0.528	1420.0	2.40	33398	67550	100948	0.889	1.411
P-203	[13] TBF/Kerosene	2.918	952.0	4.00	37318	67550	104868	5.100	8.096
P-301	[20] Post-stripping	19.112	878.9	0.61	5254	67550	72804	23.191	36.810
P-302	[21] Oxalic Feed	0.034	1650.0	0.61	9864	67550	77414	0.043	0.069

III.E.5 Filters

The filters used throughout the process are designed to separate incoming solid and liquid products. To accomplish this, conveyor belt filters are utilized. These filters leach liquids from a passing slurry through the use of a vacuum. The necessary surface area and power associated with these filters to accomplish the necessary separation is given in **Table III.E.5-1** below. F-201 is not a belt filter, but instead a grit filter designed to remove any solid impurities from the system at that point.

Table III.E.5-1. Belt Filter Data

Filter	Feed Stream	Incoming Flow (m^3/hr)	A (m^2)	ΔP (Pa)	P_{ideal}(W)	Filter Type
F-101	[3] Out of Leaching	0.06	0.30	20265	18.47	Belt Filter
F-102	[8] Out of Selective Precipitation	0.99	0.26	20265	304.82	Belt Filter
F-301	[22] Out of Oxalic Precipitation	0.18	0.16	20265	55.42	Belt Filter

IV. ECONOMICS

IV.A Anticipated Annual Revenue

The current economic viability of thorium dioxide is low since the nuclear market for it has not yet developed. As the prices for ThO_2 would likely change if it were to be produced on a large scale and used for nuclear power production, the cost for which ThO_2 could be sold is compared to that of UO_2 on a per energy basis. Uranium-235 has an energy density of 79,390,000 MJ/kg, and thorium-232 has an energy density of 79,420,000. The price of UO_2, which is formed through the conversion and enrichment of U_3O_8, is approximately $1390/kg (World Nuclear Association, 2020). Due to the energy density of thorium and uranium being incredibly similar, the final price for which ThO_2 is able to be sold is $1391/kg. The final revenue being collected from the sale of ThO_2 per every 1000 kg of monazite ore going in is $79,090. When comparing the revenue of the product to the costs of the starting materials this would be an economically advisable endeavor.

The proposed system is expected to generate $44,693,561.76 annually and is broken down in **Table IV.A.1-1**.

Table IV.A.1-1. Anticipated Annual Revenue

Component	Amount Recovered (kg/day)	Value per kg	Annual Revenue
Thorium Oxide	101.71	$1391	$42,444,417.60
Cerium Hydroxide	320.06	$1.7	$163,232.87
Lanthanum Hydroxide	178.80	$2.15	$115,376.21
Neodymium Hydroxide	106.80	$61.5	$1,970,535.08
			Total: $44,693,561.76

IV.B Purchased Equipment and Total Capital Plan Costs

IV.B.1 Major Equipment Costs

Major equipment (reaction vessels, purification columns, and storage tanks) costs were estimated with CAPCOST 2017, an Excel-based program for estimating equipment costs created by Turton et al. at West Virginia University. Vessel and storage costs were estimated assuming a maximum allowable stress of 931 atm and a weld efficiency of 0.9. Vessels were assumed to have a maximum allowable pressure of 1.2 atm.

If designed specifications were smaller than the smallest available equipment to purchase, the cost of the smallest equipment piece was used. The costs of the stripping and extraction columns were estimated by summing the CAPCOST value for a distillation column with the same number of trays and a mixer of the appropriate power. The cost of a rotary kiln was estimated in CAPCOST to be that of a gas-fired dryer with the equivalent surface area. Big bag costs for final thorium oxide storage were obtained from Uline.

Table IV.B.1-1. Purchased Equipment Cost Summary

Tag	Equipment Type	Equipment Costs	Number of Units	Total Cost
Block 1:				
V-101	Reaction Vessel	$9,100	1	$9,100
V-102	Reaction Vessel	$18,700	1	$18,700
T-101	Storage Tank	$57,700	1	$57,700
T-102	Storage Tank	$57,700	1	$57,700
T-103	Storage Tank	$246,000	1	$246,000
T-104	Storage Tank	$57,700	1	$57,700
Block 2:				
V-201	Reaction Vessel	$8,320	1	$8,320
V-202	Extraction Column	$192,800	1	$192,800
V-203	Stripping Column	$262,240	1	$262,240
T-201	Storage Tank	$57,700	1	$57,700
T-202	Storage Tank	$246,000	1	$246,000
T-203	Storage Tank	$57,700	1	$57,700
Block 3:				
V-301	Reaction Vessel	$8,320	1	$8,320
V-302	Rotary Kiln	$37,400	1	$37,400
T-301	Storage Tank	$57,700	1	$57,700
				Total: $1,711,680

IV.B.2 Pump Costs

Pump costs were estimated using CAPCOST 2017 and are summarized in **Table IV.B.4-1**.

Table IV.B.2-1. Purchased Pump Cost Summary

Tag	Equipment Type	Equipment Costs	Number of Units	Total Cost
P-101	Positive Displacement	$38,645	2	$77,290
P-103	Positive Displacement	$50,795	2	$101,590
P-104	Positive Displacement	$50,795	2	$101,590
P-105	Positive Displacement	$38,645	2	$77,290
P-201	Positive Displacement	$50,795	2	$101,590
P-202	Positive Displacement	$50,795	2	$101,590
P-203	Positive Displacement	$38,645	2	$77,290
P-301	Positive Displacement	$50,795	2	$101,590
P-302	Positive Displacement	$50,795	2	$101,590
				Total: $841,410

IV.B.3 Heat Exchanger Costs

Heat exchanger costs were estimated using CAPCOST 2017 and are summarized in **Table IV.B.4-1**.

Table IV.B.3-1. Purchased Heat Exchanger Cost Summary

Tag	Equipment Type	Equipment Costs	Number of Units	Total Cost
E-101	Fired Heater	$4,030,000	1	$40,300
E-102	Shell/Tube Heat Exchanger	$226,300	1	$226,300
E-103	Double Pipe Heat Exchanger	$32,110	1	$32,110
				Total: $298,710

IV.B.4 Filter Costs

Filter costs were estimated using information from Alibaba (2021) and are summarized in **Table IV.B.4-1**.

Table IV.B.4-1. Purchased Filter Cost Summary

Tag	Equipment Type	Equipment Costs	Number of Units	Total Cost
F-101	Belt Filter	$2,600	1	$2,600
F-102	Belt Filter	$2,600	1	$2,600
F-301	Belt Filter	$2,600	1	$2,600
				Total: $7,800

IV.B.5 Total Capital Cost of Plant

The total capital cost of the plant was estimated using the Lang Factor method, described by **Eqn. IV.B.5-1**.

$$C_{TM} = (F_{Lang}) \sum_{i=1}^{n} C_{E,i} \quad \textbf{(Eqn. IV.B.5-1.)}$$

The Lang factor for a liquids processing plant is 4.74, and is used to upper bound the cost of this plant. The major equipment costs (vessels, storage tanks, pumps, filters, and heat exchangers) of the plant are $2,859,625, yielding a total capital cost estimate of $13,554,623.

IV.C Operating Costs

IV.C.1 Raw Materials

The costs per unit of monazite and 25% ammonium hydroxide were obtained from Saleduddin, which was published in 2019. The oxalic and sulfuric acid prices were obtained from ebiochem in 2020, the nitric acid price was obtained from Fisher Scientific in 2020, the kerosene price was obtained from the Energy Information Administration in 2020, the process water price was obtained from Turton et al. (2018), and tributyl phosphate was obtained from Alibaba in 2020.

Table IV.C.1-1. Raw Materials Cost Summary

Component	Steady State Flow	Cost per kilogram	Total Cost/a
Monazite	1000 kg/day	$1.70	$510,041
Sulfuric Acid	1960 kg/day	$0.17	$101,996
Ammonium Hydroxide	21,600 kg/day	$0.25	$1,620,000
Nitric Acid	520 kg/day	$3.58	$1,014,801
Tri-butyl phosphate (TBP)	1200 kg/day	$1.10	$396,000
Kerosene	2800 kg/day	$0.41	$342,261
Oxalic Acid	80 kg/day	$0.02	$4,781
Process Water*	4073 kg/day	$0.18	$212
			Total Annual Costs: $3,990,092

*Cost is per 1000 kg

IV.C.2 Operating Labor

Operating labor is calculated via **Eqn. IV.C.2-1** from Turton et al. (2018).

$$N_{OL} = (6.29 + 31.7P_{Px}^{2} + 0.23N_{np})^{0.5} \quad \textbf{(Eqn. IV.C.2-1)}$$

Using the above equation, an estimate for the number of operators per shift could be created. Key unit operations in this process are divided into particulate and nonparticulate steps for the equation out of Turton et al. (2018) and are listed accordingly in **Table IV.C.2-1.** From these calculations, 28.3 operators per shift were required which was multiplied by 4.5 and rounded up to 125 operators required on payroll per year. A cost of $67,000 dollars per year was assumed for operators resulting in a total of $8,375,000 per year in operating labor costs. Further labor costs for the plant are estimated in the standard cost of manufacturing costs section and in **Table IV.C.5-1.**

Table IV.C.2-1 Equipment Summary for Operating Labor

Classification	Equipment	Total Number
Particulate Solids Steps	P-102 F-101 F-102 F-301 T-302	5
Nonparticulate Solids Steps	E-101 V-101 E-102 E-103 V-102 V-201 V-202 V-203 V-301 V-302 E-301	11

IV.C.3 Utilities

Major utility prices were adapted from Table 8.3 in Turton et al. (2018) and are summarized in **Table IV.C.3-1.**

Table IV.C.3-1. Standard Major Utilities Pricing

Utilities	Price	Per Unit
Cooling water	$15.7000	/ 1000 m^3
Moderately low temperature refrigerated water	$0.0172	/ kW
Water for process use	$0.1770	/ 1000 kg
Electrical substation (agitators, pumps, etc.)	$0.0674	/ kWh
Natural gas	$0.1119	/ std m^3
Pressurized air supply (add 20% for instrument air)	$0.5000	/ 100 std m^3

The necessary utilities needed for the various aspects of the process were calculated at the time of the initial design. **Table IV.C.3-2** is a summary of those calculations and translating those flows into dollar amounts.

Table IV.C.3-2. Utility Cost Summary

Equipment Tag	Utility Stream	Amount /a		Total Cost/a
General:				
	Instrument Air	300.00	100 std m^3	$150.00
Block 1:				
P-101	Sulfuric Acid Pump	21.14	kWh	$1.42
E-101	Natural Gas Fired Heater	7567.99	std m^3	$846.86
V-101	Leaching Agitator	39.92	kWh	$2.69
V-101	Cooling Water	9.24	1000 m^3	$145.03
P-103	Leaching Fluid Pump	24.88	kWh	$1.68
E-102	Cooling Water	2.40	1000 m^3	$37.67
F-101	Leaching Belt Filter	147.76	kWh	$9.96
P-104	Pre-selective Precipitation Pump	15.84	kWh	$1.07
P-105	Ammonium Hydroxide Pump	225.57	kWh	$15.20
E-103	Cooling Water	60.32	1000 m^3	$946.99
F-102	Selective Precipitation Belt Filter	2438.56	kWh	$164.36
Block 2:				
P-201	Nitric Acid Pump	6.05	kWh	$0.41
V-201	Nitric Acid Reactor Agitator	3.28	kWh	$0.22
V-201	Cooling Water	0.50	1000 m^3	$7.88
P-202	Nitrate Pump	10.16	kWh	$0.68
P-203	Solvent Pump	58.29	kWh	$3.93
V-202	Extraction Column Disc Rotation	912.32	kWh	$61.49
V-203	Stripping Column Disc Rotation	1520.56	kWh	$102.49
Block 3:				
P-301	Pre-precipitation Pump	265.04	kWh	$17.86
P-302	Oxalic Acid Pump	0.49	kWh	$0.03

V-301	Precipitation Agitator	116.64	kWh	$7.86
V-301	Water Refrigeration	64827.76	kWh	$1,113.22
V-301	Refrigerated Water Flow	0.03	1000 m^3	$0.47
F-301	Precipitation Filter	443.36	kWh	$29.88
V-302	Kiln	13983.80	kWh	$942.51
				Total Costs: $4,611.87

IV.C.4 Waste

Calculations for waste disposal costs are taken from Turton et al. (2018). Nonhazardous solid and liquid waste disposal is priced at $36 per tonne. This estimate includes waste streams 14 and 19, which contain negligible amounts of radioactive elements. Wastewater treatment is $56 per 1000 m^3 for tertiary treatment which includes filtration, activated sludge, and chemical processing, and is employed for stream 23. Gaseous waste is vented to the atmosphere.

Two radioactively significant waste streams are present in this plant: stream 4, which is composed of unreacted phosphate materials, and stream 9 where a majority of the rare earths from this process are isolated. The World Nuclear Association (2020) classifies monazite sand as a naturally occurring radioactive material (NORM), which radiation levels low enough to be considered very low-level waste (VLLW). This material poses no immediate threat to the people or surrounding environment, and has no unique disposal procedures. Hazardous waste disposal is priced at $1500 per tonne in Turton et al. (2018). Waste stream 9 has economic value due to its high concentration of rare earths, and can be sold to other plants for treatment once the solid products are filtered. The plant's overall waste costs are shown in **Table IV.C.4-1,** and were found to be $430,361.

Table IV.C.4-1. Waste Stream Cost Estimates

Stream Tag	Waste Stream	Amount/a	Total Cost/a
4	Leaching Solid Waste	30 tonnes	$45,144
9	Rare Earth Slurry	7,300 tonnes	$262,800
14	Extraction Aqueous Waste	1,469 tonnes	$52,860
19	Stripping Solid Waste	NNF	N/A
23	Oxalic Liquid Waste	1,242 m^3	$69,556
			Total: $360,874

IV.C.5 Standard Cost of Manufacturing

The standard cost of manufacturing (C_{OM}) is used to estimate the manufacturing costs of a chemical product by incorporating several different elements. These elements can be broken into three categories, as can be found in Table 8.1 in Turton et al. (2018). Direct costs are factors that vary with the rate of production of the chemical product. Fixed costs are costs that do not vary with the rate of production. General expenses are costs not related to the process directly, but instead concern management-level and administrative activities that are still necessary. The values for estimation included in **Table IV.C.5-1** were adapted from Table 8.2 in Turton et al. (2018). The fixed capital investment (*FCI*) for the purpose of this table was estimated to be equal to C_{TM} as calculated in **Eqn.IV.B.5.1.**

Table IV.C.5-1. Cost of Manufacturing Summary

Cost Type	Estimation/Equation	Total Cost/a
Direct Costs:		
Raw Materials	C_{RM}	$3,990,092
Waste Treatment	C_{WT}	$360,874
Utilities	C_{UT}	$4,612
Operating Labor	C_{OL}	$8,375,000
Direct Supervisory and Clerical Labor	0.18 C_{OL}	$1,507,500
Maintenance and Repairs	0.06 *FCI*	$813,277
Operating Supplies	0.009 *FCI*	$121,992
Laboratory Charges	0.15 C_{OL}	$1,256,250
Patent and Royalties	0.03 *COM*	$919,828
Fixed Costs:		
Depreciation	0.1 *FCI*	$1,355,462
Local Taxes and Insurance	0.032 *FCI*	$433,748
Plant Overhead Costs	0.708 C_{OL} + 0.036 *FCI*	$6,417,466
General Manufacturing Expenses:		
Administration Costs	0.177 C_{OL} + 0.009 *FCI*	$1,604,367
Distribution and Selling Costs	0.11 *COM*	$3,372,704
Research and Development	0.05 *COM*	$1,533,047
		Total: $30,660,944
		Total with Depreciation: $32,016,406

IV.D Cash Flow Analysis

IV.D.1 Working Capital

It is assumed that in the first year of operation, the plant will have some additional capital costs. These anticipated costs will be covered by an additional investment of funds called working capital. This working capital will cover the usual first year operating costs such as equipment failures, start-up raw materials, and additional labor costs. Based on the estimation techniques presented in Turton et al. (2018), a working capital total of 20% of the fixed capital investment will be spent in the final year of construction. The working capital will therefore total $2,710,924.50.

IV.D.2 Depreciation

A five year MACRS depreciation method was used for this process as recommended in Turton et al. (2018). Using this method, depreciation is applied to the fixed capital investment for a different amount each year the depreciation is in effect. The first year is 20%, the second 32%, the third 19.2%, the fourth and fifth are 11.52%, and the last year is 5.76%. This method is an accelerated depreciation method which allows the fixed capital investment to be discounted through federal tax law.

IV.D.3 Taxes

A total tax rate of 41% was estimated for this process and applied to the net revenue to obtain profit values. Net taxable income for this project approaches the highest federal income tax rate of 35% according to Turton et al. (2018) so this tax rate was assumed as an upper bound. An additional 6% in taxes would come from local and state taxes in Virginia to reach the total of 41% (Virginia Department of Taxation, 2021). A point of further study would be to add tax credits for green energy projects that this process may qualify for.

IV.D.4 Non-discounted Cash Flow

Non-discounted cash flow analysis shows how much money the plant makes each year without accounting for a discount rate. Investment costs, taxes, and depreciation are all still used in this analysis. A two year construction time was assumed for this project followed by twelve years of operation so the total project lifetime is fourteen years (Lin, 2018). Based on these assumptions and those stated in previous sections, the net cash flow each year is presented in **Table IV.D.4-1.**

Table IV.D.4-1. Non-discounted Cash Flow in Millions of USD

Year	Investment (M)	Depreciation (M)	Revenue (M)	Operating Cost (M)	Net Profit (M)
0	$1.80	$0.00	$0.00	$0.00	-$1.80
1	$6.78	$0.00	$0.00	$0.00	-$6.78
2	$9.49	$0.00	$0.00	$0.00	-$9.49
3	$0.00	$10.84	$44.69	$30.66	$9.39
4	$0.00	$6.51	$44.69	$30.66	$10.06
5	$0.00	$3.90	$44.69	$30.66	$9.35
6	$0.00	$2.34	$44.69	$30.66	$8.92
7	$0.00	$0.78	$44.69	$30.66	$8.92
8	$0.00	$0.00	$44.69	$30.66	$8.60
9	$0.00	$0.00	$44.69	$30.66	$8.28
10	$0.00	$0.00	$44.69	$30.66	$8.28
11	$0.00	$0.00	$44.69	$30.66	$8.28
12	$0.00	$0.00	$44.69	$30.66	$8.28
13	$0.00	$0.00	$44.69	$30.66	$8.28
14	$0.00	$0.00	$44.69	$30.66	$8.28
				Cumulative Profit:	**$86.84**

IV.E Profitability Analysis

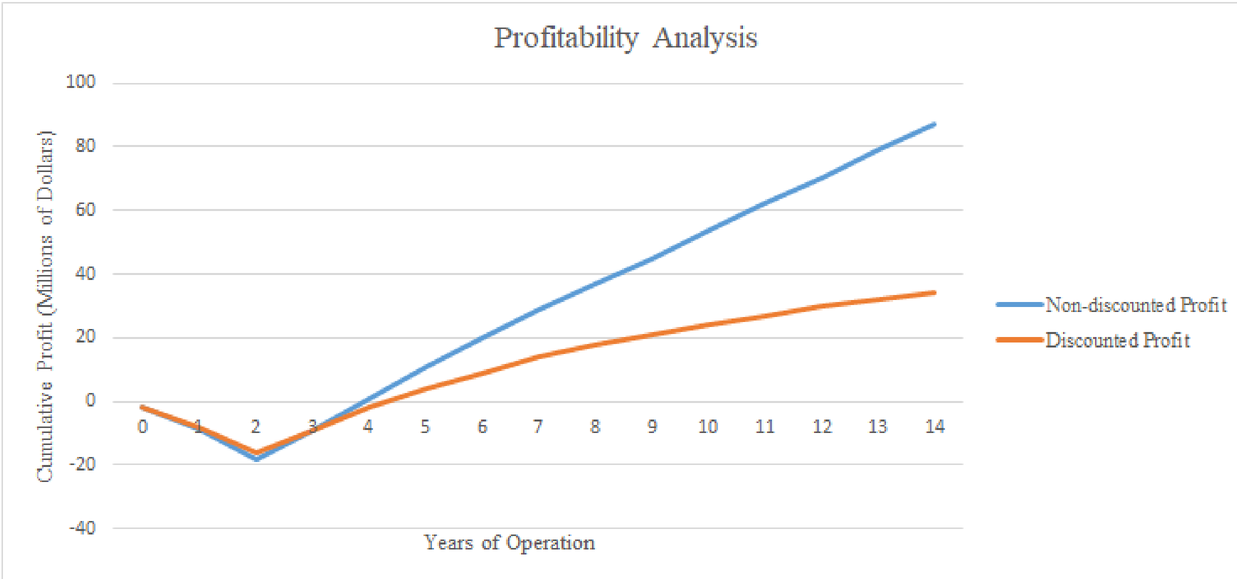

Figure IV.E.1-1: Cumulative profit over plant lifetime.

Figure IV.E.1-1 shows how the cumulative profit of the plant changes over time. Both the non-discounted and discounted profit lines break even shortly before the fourth year of the project and the plant is not expected to lose money in any year after construction is completed. The discounted profit assumes a discount rate of 10% and cumulatively generates \$34,370,000 when the project is completed after 14 years. The profitability of the project can be further shown through an analysis of the internal rate of return (IRR). The value of IRR is represented by variable r in **Eqn. IV.E.1-1** and is the discount rate at which the net present value (NPV) of the entire project is equal to zero.

$$0 = NPV = \sum_{n=0}^{N} \left(\frac{CF_n}{(1+r)^n}\right) \quad \textbf{(Eqn.IV.E.1-1)}$$

The IRR for this project was determined to be 40.39% over 14 years which indicated that this project is comfortably profitable under the assumptions that have been made. Based on this analysis, the project is a good economic opportunity and would be expected to turn a profit in its lifetime. No salvage is expected to provide a significant return at the end of this project but the land could be sold for its original value of \$1,800,000 (Crexi, 2021).

IV.G Economic Summary

Overall, this project is expected to yield \$34,370,000 of profit over 14 years and would be a good economic opportunity. The vast majority of the revenue comes from the thorium oxide being sold \$42,444,417.60 each year with money generated from viable waste streams providing another \$2,249,144.16 for a total of \$44,693,561.76 in revenue. Manufacturing costs totaled \$30,660,944 with the bulk of operating costs coming from labor. Non-discounted annual profit leveled out at \$8,279,245 after an assumed tax rate of 41% and the IRR was determined to be 40.39% over the lifetime of the plant. All of these numbers are based on the fact that thorium could one day be as valuable as uranium on an energy basis and this analysis shows a promising investment opportunity under that scenario.

V. ENVIRONMENTAL CONSIDERATIONS

V.A Block 1: Thorium Isolation

V.A.1 Sulfuric Acid Leaching Waste

The first waste stream in the process is in the form of unreacted solids filtered after the sulfuric acid leaching reaction in V-101. Stream 4 leaving leaching filter F-101 contains only 4.167 kg/hr of solids each hour. In this simplified process where reactants are only thorium, cerium, lanthanum, and neodymium, the waste stream is listed as being made up of entirely these materials with the composition at which they appear in monazite. In actuality, the make up of this stream may include unexpected contaminants which naturally occur in monazite. This uncertainty discourages simply recycling the stream back through V-101 and makes it difficult to suggest stream 4 as being saleable. Radioactive components have not been specifically separated from the stream at this point of the process so the waste would be considered low-level radioactive waste (Heimberg, 2017). A facility for processing and storing such waste exists in Barnwell, South Carolina and is the choice for stream 4 waste disposal.

V.A.2 Selective Precipitation Waste

Stream 9 out of selective precipitation belt filter F-102 is the next waste stream for the process and is the most saleable waste stream. This stream leaves with a much higher concentration of rare earth metals that were separated from the thorium concentrated solids and each of these elements has a potential vendor. Cerium, lanthanum, and neodymium are found in the highest concentrations in this waste stream but trace amounts of other elements are also present. This waste stream is also where trace amounts of uranium exit the process and contributes to it being low-level radioactive waste. Nevertheless, the stream still provides economic opportunity. In one scenario, further rare earth processing plants could be built adjacent to this one focused on thorium. Detailed analysis of these steps are outside the scope of this thesis but rare earth element processing is a much more established field than thorium processing. This scenario also makes sense because of how much of monazite's composition is these rare earth elements. Alternatively, the waste stream could be transported to an existing processing facility. Some processing would still be required on site since the majority of the 1013.89 kg/hr stream is water. Separating this water would make the waste much more affordable to transport great distances and would certainly be necessary.

V.B Block 2: Thorium Purification

V.B.1 Extraction Waste

Stream 14 out of extraction column V-202 is a mixture of an aqueous phase with a significant organic phase of TBP in kerosene accompanying it. Both phases contain similar amounts of thorium, cerium, lanthanum, and neodymium at flow rates of less than 1 kg/hr within a total flow rate of 203.93 kg/hr. Unlike the waste stream leaving the precipitation vessel, the separation of elements in this stream would be a much more complicated process. If this path were to be accomplished, further processing would have to be onsite to separate the complicated mixture. The more likely option would be to simply dispose of the mixture. As a low-level radioactive waste stream, the mixture would be sent to a processing and storage facility like the one in South Carolina. Considering the cost of constructing processing onsite for low concentration of rare earth elements, storage is almost certainly the more viable option.

V.B.2 Organic Stripping Waste

Stream 19 out of filter F-201 is a stream of negligible flow rate on an hourly basis. Nevertheless, some accumulation of solids is expected over time suspended in the aqueous stream leaving the stripping vessel. This accumulation could consist of cerium, lanthanum, neodymium, other rare earth elements, or other unexpected products of the process. Due to the uncertainty of this waste stream, the safest bet is on waste disposal to a low-level radioactive waste site.

V.C Block 3: Thorium Oxide Formation

V.C.1 Oxalate Precipitation Waste

Stream 23 out of oxalate precipitation belt filter F-301 is a liquid waste stream that is almost entirely water with a small amount of nitric acid and oxalic acid. This stream contains no rare earths or thorium oxalate in it so it is not a saleable product. The acids within the stream could potentially be recycled back into the process but this would require separation equipment and would not be economically viable for the small amount of acid. Much of the fluid has been alongside radioactive material for the past few hours of processing so this stream should be considered to be low-level radioactive waste. As a result, the 172.51 kg/hr waste stream should be sent to an appropriate processing and storage facility.

V.C.2 Calcination Waste Gas

The last waste stream leaving the processing plant is waste gas stream 25 leaving calcination kiln V-302. A total of 3.75 kg/hr of gas leaves the vessel with a mixture of water, carbon monoxide, carbon dioxide, and other combustion gases. To ensure only carbon dioxide and water are leaving the system, the gas is sent through a catalytic converter to guarantee complete conversion. The carbon leaving this process is negligible compared to the energy density of the carbon free fuel provided by thorium dioxide.

VI. SAFETY CONSIDERATIONS

VI.A Chemical Hazards and Compatibility

The different chemicals used throughout the process pose significant hazards that must be taken into account. Monazite is a highly toxic substance via inhalation and ingestion, and targets the kidney, liver, lungs, and brain, all non-essential organs. It is also dangerous though absorption and is carcinogenic. Sulfuric, oxalic, and nitric acid are highly corrosive and can cause severe damage to skin and eye and can irritate the lungs if inhaled. Nitric acid is also an oxidizer and can intensify flammable conditions. Ammonium hydroxide is corrosive and is toxic if absorbed, ingested, or inhaled. Kerosene is a flammable liquid and vapor that poses explosive and flammable risks. Additionally, it is toxic if absorbed, ingested, or inhaled. Tributyl phosphate causes skin and eye irritation, is harmful if ingested, and is carcinogenic. Ammonium hydroxide, tributyl phosphate, and oxalic acid also pose serious environmental risks to aquatic and terrestrial life. Similar to monazite, thorium oxide, the final product, is very toxic and carcinogenic.

The chemicals used in the process are very dangerous on their own, but they also pose major risks if certain combinations of chemicals are mixed outside of intended processes in designed vessels. **Figure VI.A-1** shows a chemical compatibility matrix, obtained from the Chemical Reactivity Worksheet, which was "developed by the Emergency Response Division of the National Oceanic and Atmospheric Administration (NOAA) and the Office of Emergency Management of the US Environmental Protection Agency (USEPA), in collaboration with the Dow Chemical Company and the Center for Chemical Process Safety (2020)." Sulfuric and nitric acids pose the greatest risk due to their ability to do complex chemistry with a variety of other chemicals. They can react with ammonium hydroxide to produce acidic and basic fumes as well as harmful pollutant nitrogen oxide (NO_x) gases, and with tributyl phosphate to form flammable alcohols and hydrocarbons. Nitric acid can also react with oxalic acid to produce NO_x while sulfuric can react with it to form sulfur oxides (SO_x) which can lead to acid rain. The purpose of the compatibility matrix is not to understand the chemistry if small amounts of the chemicals come into contact with one another, but what could occur if large amounts are inadvertently put into the same tank or if spills result in large volumes of chemicals interacting with one another. Additionally, the figure also shows the National Fire Protection Association (NFPA) hazards for each of the chemicals, which would be important for operators and emergency response workers to be aware of.

Y : Compatible
N : Incompatible
C : Caution
SR : Self-Reactive
*: Changed by user

NFPA				Thorium Compatibility Chart	AMMONIUM HYDROXIDE	KEROSENE	NITRIC ACID, RED FUMING	OXALIC ACID	SULFURIC ACID	TRIBUTYL PHOSPHATE	WATER
Health	Flammability	Instability	Special								
				AMMONIUM HYDROXIDE							
2	2	0		KEROSENE	Y						
4	0	1	Oxi	NITRIC ACID, RED FUMING	N	N					
3	1	0		OXALIC ACID	C	Y	N				
3	0	2	No	SULFURIC ACID	N	N	C	N			
3	1	0		TRIBUTYL PHOSPHATE	C	Y	N	Y	N		
				WATER	C	Y	C	Y	C	C	

Figure VI.A-1 Chemical Compatibility Matrix

VI.B Radiation Hazards

The quantifiable radiation health hazards are evaluated using Sieverts, which measures the radiation a human receives per unit mass. According to the Nuclear Regulatory Commission, 50 mSv is the annual dose limit for radiation workers. Monazite sands are radioactive and carcinogenic and are dangerous if they are inhaled or ingested. A study by Iwaoka et al. found that for a monazite processing plant, workers received a dose of 0.62 mSv, which is far lower than the standard (Iwaoka et al., 2017). Of the total dose, 0.43 mSv was from external contact while the remaining 0.19 was due to inhalation. Because alpha particles are low-penetrating and workers will wear long clothes, the external dose will be minimized. To mitigate dust inhalation, the concrete monazite storage will be closed as often as possible and when entering, workers will be required to wear masks. Additionally, depending on the method that the monazite is delivered to the site, the area will need to be cleaned regularly to prevent accumulation of dust. Similar cautions should be taken in regards to thorium oxide storage. Overall, the radiation hazards at the plant are minimal and the inherent toxicity of the materials pose a greater risk.

VI.C Explosion, Burn, and Mechanical Hazards

The only flammable substance present in the process is kerosene, so fire and explosive hazards are minimal, though operators should wear flame resistant clothing (FRC). Of course, if a fire were to break out next to a tank, the risk of a boiling liquid expanding vapor explosion (BLEVE) is still possible if the pressure within a tank exceeds the maximum allowable working pressure (MAWP). Natural gas is used to heat up the sulfuric acid in a fired heater, so appropriate maintenance and operation are essential in the prevention of a leak or explosion. The leaching process equipment at 230ºC should be covered in insulation to prevent operators from burning themselves and to prevent heat loss. The risk of dust explosion should always be evaluated when working with powdered substances, but fortunately monazite and thorium oxide are not combustible, so there is no risk of a combustible dust explosion.

A major concern for the process is the high numbers of exothermic reactions occurring. If the flow of cooling water to a vessel or pipe jacket was to fail, a runaway reaction could occur, increasing the pressure inside the vessel and leading to an explosion. As such, there should not only be a redundant cooling water supply, but all process vessels should be fitted with a pressure relief valve (PRV) that opens when the pressure in the vessel becomes too high. In addition, rupture discs should be installed in tandem with the PRVs to improve the reliability of the valve because of the corrosive nature of many of the reactions.

Positive displacement pumps discharge a constant volume, so a PRV is required at the discharge line in the event that there is a blockage or closed valve in the piping ahead. The PRV discharge does not necessarily need to transfer the excess liquid to another location; it can actually recirculate the liquid to the suction line of the pump, or pumps with built-in recirculating PRVs could be used to simplify the process.

The conveyors and filters have belts which pose a mechanical hazard. To prevent the risk of an incident, operators should keep their hands away from moving parts, and when maintenance is being performed, a complete lock out tag out (LOTO) process must be established to prevent the conveyors from accidentally restarting and catching extremities in machinery.

VI.D Safety Culture

One of the most important aspects of minimizing the probability of an accident is a strong safety culture. Culture can be defined as “the shared values and beliefs that interact with an organization's structures and control systems to produce behavioral norms” (Unnerstall, 2020). Applying this idea of company culture to safety can allow for important questions to be asked as well as preventing incidents when leading warning signs display themselves. This safety culture should be visible in all levels of the organization. Company leadership should reinforce safety as both a priority and value. There should also be a climate throughout the company that enables employees to voice their concerns. Procedures should be in place to respond to those concerns raised by employees. Finally, there should be sufficient training to enable effective communication with a focus on continuous improvement (Unnerstall, 2020). These steps, and others not mentioned, should allow for an effective safety culture to be established.

VII. SOCIAL CONSIDERATIONS

VII.A Employment

The number of operators needed per shift was calculated using **Eqn. IV.C.2-1.** The number of steps in the process where solids must be directly handled, P_{Px}, is equal to five. There are four filters dealing with solids in this process and then the solid feed and product at each end of the process. The rest of the processes, N_{np} , total eleven steps of heat exchangers, reactors, or columns. Using the formula from Turton, twenty-nine operators would be required for this plant each shift. Multiplying by 4.5 gives the year round total of 125 operators employed by this process. Using the same estimation techniques used in Turton et al. (2018), about 120 other employees in a variety of non-operator positions are required for the plant to run. These estimates indicate that 213 jobs will be provided to the community within which the plant is sited. These jobs are an economic incentive to the community that accepts the safety risk associated with this process. How the incentive of jobs compares to the potential risks depends on the community and what industry risks may already be normalized.

VII.B Plant Siting

Since scale up calculations are based in Virginia, the processing plant is as well. Virginia is currently home of two nuclear power plants, both of which were built in the 1970s and are now approaching the end of their expected lifespan. The Surry Nuclear Power Plant is the older of the two and was commissioned in 1973. When its lifetime is complete, a decision will have to be made about how to replace that source of energy and a thorium reactor could be that replacement if it proves to be the next generation of nuclear power. This region of Virginia has proven to be viable for nuclear power processes already and there is no reason to believe it would not in the future. Therefore, either Surry or Isle of Wight counties in Virginia are reasonable choices for a location of a monazite processing plant. Transportation costs of both product and raw materials could be minimized due to the proximity to ports and previous nuclear projects. The region's history also helps reduce the safety concerns communities might have with a processing plant for radioactive material.

VII.C Political Impacts

In the United States, energy policy is increasingly focused around resilience and independence. Having domestic nuclear power plants that are on the cutting edge of new technology and efficiency would fit well into these goals. The advent of novel thorium reactors could be the push required for the U.S. to construct new nuclear power plants. While the U.S. does not currently mine its monazite resources, thorium reactor technology could change this. Domestically produced monazite offers another incentive for a monazite processing plant and provides the potential for a new energy source with an entirely American supply chain. Without locally produced monazite, South African monazite is the next likely option. Ultimately, there are several barriers for a monazite processing plant to become politically appealing, but the prospect of substantial, domestic energy may garner support.

VIII. FINAL RECOMMENDED DESIGN

VIII.A.Block 1: Thorium Isolation Specifications

VIII.A.1 Thorium Isolation Equipment Overview

Block 1 requires 3 feed storage tanks, 1 jacketed agitated reactor, 1 jacketed selective precipitation vessel, 2 filters, 3 heat exchangers, 4 pumps, 1 conveyor, and 1 intermediate storage tank. A list of every major piece of equipment purchased for Block 1 and their relevant streams is included in **Table VIII.A.1-1**.

Table VIII.A.1-1 Block 1 Equipment

Equipment ID	Name	Relevant Streams
T-101	Sulfuric Acid Storage Tank	1
P-101	Sulfuric Acid Pump	1
E-101	Leaching Pre-Heat	1
T-102	Monazite Sand Storage Tank	2
P-102	Monazite Conveyor	2
V-101	Leaching Vessel	1, 2, 3
P-103	Leaching Fluid Pump	3
E-102	Leaching Cool-Down	3
F-101	Leaching Filter	3, 4, 5
P-104	Pre-Selective Precipitation Pump	5
T-103	Ammonium Hydroxide Storage Tank	6
P-105	Ammonium Hydroxide Pump	6
E-103	Selective Precipitation Mixing Cooling Jacket	5, 6, 7
V-102	Selective Precipitation Vessel	7, 8
F-102	Selective Precipitation Filter	8, 9, 10
T-104	Block 1 Intermediate Storage	10

VIII.A.2 Sulfuric Acid Leaching Equipment Summary

The equipment summary for the Sulfuric Acid Leaching is given in **Table VIII.B.2-1**.

Table VIII.A.2-1 Equipment Summary for Sulfuric Acid Leaching

Equipment ID	Name	Design Specifications
T-101	Sulfuric Acid Storage Tank	MOC: Carbon Steel Capacity: 15.22 m^3
P-101	Sulfuric Acid Pump	Differential Pressure: 1.47 bar Power Consumption: 2.94 W Flow Rate: 0.8 L/min
E-101	Leaching Pre-Heat	Gas Requirement: 1.05 m^3/hr MOC: Carbon Steel
T-102	Monazite Sand Storage Tank	MOC: Concrete Capacity: 2.69 m^3
P-102	Monazite Conveyor	Flow Rate: 41.67 kg/hr
V-101	Leaching Vessel	MOC: Stainless Steel Temperature: 230^{o}C Pressure: 1 atm Flow Rate: 125 kg/hr Capacity: 100 gal Diameter: 0.67 m Height: 1.1 m Cooling water flow rate: 1283 kg/hr Impeller: 3 blade hydrofoil w/ 22% solidity ratio Impeller diameter: 0.3 m Impeller width: 0.04 m Impeller speed: 64 RPM Power: 4.99 W Number of baffles: 4 Baffle width: 0.06 m
P-103	Leaching Fluid Pump	Differential Pressure: 1.35 bar Power Consumption: 3.46 W Flow Rate: 1 L/min
E-102	Leaching Cool-Down	MOC (Tubes): Stainless Steel MOC (Shell): Stainless Steel Water Flow Rate: 333.3 L/hr Number of Tubes: 6 Tube Passes: 2
F-101	Leaching Filter	Area: 5.8 m^2 Power: 4 kW

VIII.A.3 Selective Precipitation Equipment Summary

The equipment summary for the Sulfuric Acid Leaching is given in **Table VIII.A.3-1**.

Table VIII.A.3-1 Equipment Summary for Selective Precipitation

Equipment ID	Name	Design Specifications
P-104	Pre-Selective Precipitation Pump	Differential Pressure: 0.872 bar Power Consumption: 2.20 W Flow Rate: 1 L/min
T-103	Ammonium Hydroxide Storage Tank	MOC: Carbon Steel Capacity: 311.75 m^3
P-105	Ammonium Hydroxide Pump	Differential Pressure: 0.765 bar Power Consumption: 31.3 W Flow Rate: 16 L/min
E-103	Selective Precipitation Mixing Cooling Jacket	MOC (Tube): Stainless Steel MOC (Shell): Carbon Steel Water Flow Rate: 139.6 L/min
V-102	Selective Precipitation Vessel	MOC: Stainless Steel Temperature: 35ºC Pressure: 1 atm Flow Rate: 1019.2 kg/hr Capacity: 2 m^3 Diameter: 0.95 m Height: 2.85 m
F-102	Selective Precipitation Filter	Area: 98.8 m^2 Power: 80 kW
T-104	Block 1 Intermediate Storage	MOC: Carbon Steel Capacity: 1.40 m^3

VIII.B Block 2: Thorium Purification Specifications

VIII.B.1 Thorium Purification Equipment Overview

Block 2 requires 2 feed storage tanks, 1 jacketed agitated mixer, 2 disk and donut separation columns, 1 filter, 3 pumps, and 1 intermediate storage tank. A list of every major piece of equipment purchased for Block 2 and their relevant streams is included in **Table VIII.B.1-1**.

Table VIII.B.1-1 Block 2 Equipment

Equipment ID	Name	Relevant Streams
T-201	Nitric Acid Storage Tank	11
P-201	Nitric Acid Pump	11
V-201	Pre-Extraction Mixer	10, 11, 12
P-202	Extraction Pump	12
V-202	Extraction Column	12, 13, 14, 15, 16
T-202	Solvent Storage Tank	13
P-203	Solvent Pump	13
V-203	Stripping Column	15, 16, 17, 18
F-201	Extraction and Stripping Filter	18, 19, 20
T-203	Block 2 Intermediate Storage	20

VIII.B.2 Conversion to Nitrates Equipment Summary

The equipment summary for the Conversion to Nitrates is given in **Table VIII.B.2-1**.

Table VIII.B.2-1 Equipment Summary for Conversion to Nitrates

Equipment ID	Name	Design Specifications
T-201	Nitric Acid Storage Tank	MOC: Stainless Steel Capacity: 8.78 m^3
P-201	Nitric Acid Pump	Differential Pressure: 0.729 bar Power Consumption: 0.841 W Flow Rate: 0.5 L/min
V-201	Pre-Extraction Mixer	MOC: Stainless Steel Temperature: 50°C Pressure: 1 atm Flow Rate: 45.01 kg/hr Capacity: 0.28 m^3 Diameter: 0.34 m Height: 0.34 m Cooling water flow rate: 69.71 kg/hr Impeller: Six Blade Rushton Turbine Impeller diameter: 0.24 m Impeller width: 0.030 m Impeller speed: 239 RPM Power: 0.41 Watts Number of baffles: 4 Baffle width: 0.029 m

VIII.B.3 Stripping and Extraction Equipment Summary

The equipment summary for Stripping and Extraction is given in **Table VIII.B.3-1**.

Table VIII.B.3-1 Equipment Summary for Stripping and Extraction

Equipment ID	Name	Design Specifications
P-202	Extraction Pump	Differential Pressure: 1.01 bar Power Consumption: 1.41 W Flow Rate: 0.6 L/min
V-202	Extraction Column	MOC: Stainless Steel Column Height: 2.40 m Column Diameter: 0.74 m Tray Spacing: 0.18 m Number of Trays: 24 Theoretical Stages: 3 Volume of Column: 1.03 m^3 Power: 114.04 W Residence Time: 0.95 hr
T-202	Solvent Storage Tank	MOC: Carbon Steel Capacity: 58.83 m^3
P-203	Solvent Pump	Differential Pressure: 1.05 bar Power Consumption: 8.10 W Flow Rate: 3 L/min
V-203	Stripping Column	MOC: Stainless Steel Column Height: 4.00 m Column Diameter: 0.71 m Tray Spacing: 0.1 m Number of Trays: 40 Theoretical Stages: 5 Volume of Column: 1.57 m^3 Power : 190.07 W Residence Time: 1.58 hr
F-201	Extraction and Stripping Filter	MOC: Stainless Steel
T-203	Block 2 Intermediate Storage	MOC: Carbon Steel Capacity: 1.40 m^3

VIII.C Block 3: Thorium Oxide Formation Specifications

VIII.C.1 Thorium Oxide Formation Equipment Overview

Block 3 requires 1 feed storage tank, 1 agitated precipitation vessel, 1 rotary kiln, 1 heat exchanger, 1 filter, 2 pumps, and 1 product storage vessel. A list of every major piece of equipment purchased for Block 3 and their relevant streams is included in **Table VIII.C.1-1**.

Table VIII.C.1-1 Block 3 Equipment

Equipment ID	Name	Relevant Streams
P-301	Pre-Precipitation Pump	20
T-301	Oxalic Acid Storage Tank	21
P-302	Oxalic Acid Pump	21
V-301	Precipitation Vessel	20, 21, 22
F-301	Precipitation Filter	22, 23, 24
V-302	Rotary Calcination Kiln	24, 25, 26
P-303	Thorium Oxide Conveyor	26
T-302	Thorium Oxide Storage	26

VIII.C.2 Oxalate Formation and Precipitation Equipment Summary

The equipment summary for Oxalate Formation and Precipitation is given in **Table VIII.C.2-1**.

Table VIII.C.2-1 Equipment Summary for Oxalate Formation and Precipitation

Equipment ID	Name	Design Specifications
P-301	Pre-Precipitation Pump	Differential Pressure: 0.728 bar Power Consumption: 36.8 W Flow Rate: 20 L/min
T-301	Oxalic Acid Storage Tank	MOC: Carbon Steel Capacity: 0.68 m^3
P-302	Oxalic Acid Pump	Differential Pressure: 0.774 bar Power Consumption: 0.069 W Flow Rate: 0.05 L/min
V-301	Precipitation Vessel	MOC: Stainless Steel Temperature: 10C Pressure: 1 atm Flow rate: 174.4 kg/hr Capacity: 75 gal Diameter: 0.61 Height: 0.98 Impeller: 6-blade Rushton Turbine Impeller diameter: 0.429 m Impeller width: 0.053 Impeller speed: 66 rpm Power: 14.58 W Number of baffles: 4 Baffle width: 0.051
F-301	Precipitation Filter	

VIII.C.3 Calcination Equipment Summary

The equipment summary for Calcination is given in **Table VIII.C.3-1**.

Table VIII.C.3-1 Equipment Summary for Calcination

Equipment ID	Name	Design Specifications
V-302	Rotary Calcination Kiln	MOC: Carbon Steel Temperature: 900 ℃ Pressure: 1.01 bar Flow Rate: 8.00 kg/hr Capacity: 18.1 m^3 Length: 34.94 m Diameter: 0.813 m Speed: 0.5 rpm Slope: 5°
P-303	Thorium Oxide Conveyor	Flow Rate: 8 kg/hr
T-302	Thorium Oxide Storage	MOC: Woven polypropylene Capacity: 0.13 m^3

IX. CONCLUSIONS AND RECOMMENDATIONS

IX.A Conclusions

The proposed process continuously converts 300,024 kg of monazite sands to 30,513 kg of >92% thorium oxide annually and requires 85,061 kWh/a. Projected startup costs total to $2.7 million, with a non-discounted annual cash flow of $8.2 million and an IRR of 40.39% over 14 years.

This plant's development requires significant environmental, safety, and social considerations. Waste streams containing REEs must be carefully disposed of or sold to the appropriate vendors, and plant personnel must be properly equipped to handle the sands, powders, strong acids, and strong bases used in the process. The plant has the potential to create 290 new jobs and become a significant domestic source of nuclear fuel for the United States.

This plant scales up many of the batch processes previously documented in literature and combines them to form a continuous process with technical detail. While the batch or semi-batch natures of previously reported thorium isolation processes may discourage the development of monazite processing plants, this continuous, scaled design may embolden companies to invest in this process. Based on the process' positive environmental impact and economic viability, we strongly recommend its construction and operation.

IX.B Recommendations

IX.B.1 Overall Process Recommendations

We have four broad recommendations for the overall process regarding monazite sand feed composition, increased accuracy for monetary estimates, more robust chemical modeling, and scale up potential.

For this process we assumed a constant composition for our monazite sand feed. In reality this composition is likely to deviate slightly with deliveries mined from the same mine, and much more significantly with deliveries mined from different mines. For this reason, we recommend better understanding of the composition of the feed, and designing the process to be able to accommodate different flow rates accordingly.

As the process becomes more known and the set up of the different units are determined, it will be important to reexamine how labor costs may be affected, specifically the labor costs concerning handling of solids and any redundancies that may be necessary for these processes. The labor costs associated with our filters are likely greatly overestimated in this report. It is also important to note that the majority of our equipment was smaller than what is specified in CAPCOST 2017. As such, we expect the values in this report to be an overestimation and should be considered carefully when focusing on capital investments. Turning attention to the end of the process, it is likely that the cost of ThO_2 will change compared to the estimation. Our estimation is grounded in a per energy basis, and does not necessarily take into account supply and demand of the fuel. Once a market for ThO_2 is more established, a more accurate estimate can be made.

We also recommend that the physical and chemical properties of the different streams and mixtures in vessels be analyzed more carefully. This could be accomplished by utilizing a chemical modeling software such as Aspen PLUS with the OLI plugin. This additional analysis would allow for power requirements for the pumps and impeller to be more exact. This additional analysis might also adjust the metallurgy choices for the various vessels as corrosion factors are more seriously considered.

Finally, we recommend that the scale up potential of this process is examined thoroughly. As has been mentioned several times throughout this report, the scale of the process is quite small, with the limiting factor being the global supply for monazite sand. If the global supply were to increase, then a larger scale of the plant may be more desirable.

IX.B.2 Block 1: Thorium Isolation Recommendations

One potential method to improve the process yield could be the inclusion of a recycle stream out of the leaching reactor to further dissolve any remaining monazite solids. Not only would this increase the amount of thorium oxide produced, but it would also reduce the waste coming out of F-101. We recommend that a study should be done on the leaching reactor to determine what could occur if there are deviations from normal impeller operation, as this could result in non-ideal mixing and an accumulation of heat in the center of the vessel that the cooling water can not effectively manage. Hence, we recommend the consideration of implementing a cooling coil within the reactor to help maintain isothermal conditions in the event of a deviation.

We recommend pursuing partnerships with other chemical production companies that would typically extract the other rare earth elements present in monazite sand instead of thorium, namely cerium, lanthanum, and neodymium. The majority of these rare earths are removed from the process in stream 9 after the selective precipitation as hydroxides. Selling this waste stream to other companies would allow for additional revenue and less waste.

We strongly recommend further metallurgical studies on the ammonium hydroxide mixing pipe, as the combination of acids, reactions, and precipitation would put the pipe walls under corrosive and erosive conditions.

IX.B.3 Block 2: Thorium Purification Recommendations

A disk and donut extraction system and a recycle ratio of 5.0 was selected for this process based on assumption from literature. Further investigation into how different extraction and recycle parameters affect the resolution of thorium nitrate separation could yield a more efficient system. Additionally, the waste stream leaving the extraction column does have some economic value to it but is not considered saleable in this economic analysis. Using less solvent while still achieving a high enough purity may be possible and would create a waste stream with a higher concentration of valuable metals.

We think it would be wise to consider adding a filter on stream 12 coming out of V-201, the pre-extraction mixer, to ensure that no solids are transferred into the stripping and extraction columns. This would decrease potential clogging in the columns themselves, thereby decreasing the necessary maintenance.

IX.B.4 Block 3: Thorium Oxide Formation Recommendations

Both the oxalate precipitation and calcination steps necessary for thorium oxide formation utilized parameters from literature due to their historical efficacy. Further investigation into these variables may be able to maintain high purities while saving on costs. The oxalate precipitation in this plant requires a low operating temperature of 10 ℃, which requires a refrigeration unit to achieve. Experimentation may find that this temperature is unnecessary, removing the need for refrigeration and saving on operating costs. Additionally, the cost of equipment utilized in this section was priced higher than reality due to their relatively minute scale. More accurate cost estimates can be made by interfacing directly with vendors or by scaling up production entirely to match industry equipment size standards.

X. ACKNOWLEDGEMENTS

We gratefully acknowledge Mr. Eric W. Anderson of the chemical engineering department at the University of Virginia for his assistance and advising throughout the project. In addition, we would like to acknowledge the capstone team of Jonathan Zheng, Matthew Denecke, Rachel Ho, and Caitlin Rudy, as their report provided invaluable organizational guidance for this report. The team would also like to acknowledge Frank Herbert for his work *Dune* for providing great conversation while completing this project. We would also like to appreciate the release of the Snyder cut of *Justice League*, as that one scene with Barry saving ~~Iris~~ the universe really is the best thing in the world.

#RestoreTheSnyderVerse

XI. TABLE OF NOMENCLATURE

Table XI.A.1-1. Table of Nomenclature

Symbol	Unit	Description
$\boldsymbol{\alpha}_{av}$	m/kg	Filter cake specific resistance
μ	Pa•s	Viscosity
v	m^3/hr	Volumetric flow rate
ρ	kg/m^3	Mass density
c	kg/m^3	Filter mass over filtrate volume
C_{bot}	m	Bottom impeller clearance
C_{OL}	$/a	Annual Operating Labor Costs
Cp	kJ/kg•K	Constant Pressure Heat capacity
C_{RM}	$/a	Annual Raw Material Costs
C_{top}	m	Top impeller clearance
C_{UT}	$/a	Annual Utilities Costs
Cv	kJ/kg•K	Constant Volume Heat Capacity
C_{WT}	$/a	Annual Waste Treatment Costs
d	m	Length
d_i	m	Impeller diameter
F	-	LMTD correction factor
FCI	$	Fixed Capital Investment
H	m	Liquid height
ΔH_{rxn}	kJ/mol	Heat of reaction
J	m	Baffle width
m	kg/hr	Mass flow rate
n_i	mol/hr	Molar flow rate
N_{np}	-	Number of non-particulate processes
N	RPM	Impeller speed
N_{OL}	-	Operators per shift
N_P	-	Power number
Δp	Pa	Filter pressure difference
P	kW	Motor power

P_{Px}	-	Number of particulate solid processes
P_S	W/m^3	Specific power
Q	kJ/hr	Heat duty
R	-	Heat capacity ratio
R_f	m^2K/W	Fouling factor
Re	-	Reynolds number
S	-	Temperature range ratio
t	s	Time
T	K	Temperature
T_d	m	Tank diameter
ΔT_{lm}	K	Log-mean temperature difference
U	W/m^2K	Overall heat transfer coefficient
U_0	W/m^2K	Heat transfer coefficient
V_{eff}	m^3	Effective volume
V_R	m^3	Reactor volume
W	m	Impeller width
Z	m	Tank height

XII. REFERENCES

Alareqi, W., et al. (2017). Solvent extraction of thorium from rare earth elements in monazite thorium concentrate. *Malaysian Journal of Analytical Sciences, 21*(6). doi:10.17576/mjas-2017-2106-zz

Alibaba (2021). *Belt Filter Press Price.* Alibaba. https://www.alibaba.com/showroom/belt-filter-press-price.html

Anderson, E.W. (2021). How to design a pump for CHE 4476. Document provided to students.

Bahri, C., et al. (2018). Extraction and Purification of Thorium Oxide (ThO2) from Monazite Mineral. Sains Malaysiana, *47*(8), 1873-1882. doi:10.17576/jsm-2018-4708-28

Bahri, C., et al. (2015). Advantages of liquid fluoride thorium reactor in comparison with light water reactor. AIP Conference Proceedings, 1659, 1-11. doi:10.1063/1.4916861

Balakrishna, P. (1988). Thorium oxide: calcination, compacting, and sintering. *Journal of Nuclear Materials*, *160*, 88-94. doi:10.1016/0022-3115(88)90012-8

Becke, A. D. (1993). Density‐functional Thermochemistry. III. The Role of Exact Exchange. J. Chem. Phys., *98*(7), 5648–5652. doi:10.1063/1.464913

Brady, J. (2019, April 30). As Nuclear Waste Piles Up, Private Companies Pitch New Ways To Store It. Retrieved October 22, 2020, from https://www.npr.org/2019/04/30/716837443/as-nuclear-waste-piles-up-private-companies-pitch-new-ways-to-store-it

Burkart, C., et al. (1952). Purification of thorium nitrate by solvent extraction with tributyl phosphate. *U.S. Atomic Energy Commission.*

Christensen, G. (1983). Units for Specific Resistance. *Water Pollution Control Federation, 55(4)*, 417-419

Crexi. (2021). Virginia land for sale. *Commercial Real Estate Exchange Inc.* Retrieved April 14, 2021 from https://www.crexi.com/properties?placeIds%5B%5D=ChIJzbK8vXDWTIgRlaZGt0lBTsA&types%5B%5D=Land

Demol, J., Ho, E., & Senanayake, G. (2018). Sulfuric acid baking and leaching of rare earth elements, thorium and phosphate from a monazite concentrate: Effect of bake temperature from 200 to 800 °C. *Hydrometallurgy*, *179*, 254-267. doi:10.1016/j.hydromet.2018.06.002.

Duda, W. H. (1984). Cement data book. Bauverlag.

Felder, R. M., & Rousseau, R. W. (2005). *Elementary principles of chemical processes*. Hoboken, NJ: Wiley.

Frisch, M. J., et al. (2016). Gaussian 16 Rev. C.01; Wallingford, CT.

General Industries, Inc. (2018). *Nitric Acid Storage Tanks*. GI Tanks. https://www.gitank.com/nitric-acid-storage-tanks#:~:text=Nitric%20acid%20tanks%20are%20another,carbon%20steel%20is%20not%20recommended.

Hania, P.R., & Klaassen, F.C. (2012). Thorium Oxide Fuel. *Comprehensive Nuclear Materials*, *3*, 87-108. doi:10.1016/B978-0-08-056033-5.00052-5

Heimberg, J. (2017). Low-level radioactive waste management and disposition. *The National Academies of Sciences, Engineering, and Medicine.* Retrieved from: https://www.ncbi.nlm.nih.gov/books/NBK441732/#:~:text=There%20are%20four%20commercial%20LLW,see%20Table%20D%2D1

Huttunen, M. et al. (2019). Specific energy consumption of vacuum filtration: experiential evaluation using a pilot-scale horizontal belt filter. *Drying Technology, 38(4),* 460-475

Iwaoka, K., Yajima, K., Suzuki, T., Yonehara, H., Hosoda, M., Tokonami, S., & Kanda, R. (2017). Investigation of natural radioactivity in a monazite processing plant in Japan. *Health physics*, *113*(3), 220-224. doi:10.1097/HP.0000000000000692

King, M.L. (2019, Oct 12). Mixing. Powerpoint presentation given in CHE 3321.

Lin, T. (2018). Decommissioning of a rare earth extraction plant and remediation of the NORM contaminated site. *International Atomic Energy Agency.*

McCabe W.L., Smith J.C., Harriott P. (1993). *Unit Operations in Chemical Engineering*. McGraw Hill.

Moon Fabricating Corporation. (2018, July 12). *Acid Storage Tank Fabrication Requires Special Consideration*. Moon Tanks. https://moontanks.com/acid-storage-tank-fabrication-requires-special-consideration/#:~:text=Materials%20of%20construction%20%E2%80%94%20Most%20tanks,acid%20concentration%2C%20and%20storage%20temperature.

Moore, R. L., Goodall, C. A., Hepworth, J. L., and Watts, R. A. (1957). Nitric Acid Dissolution of Thorium. *Ind. Eng. Chem.*, *49*(5), 885–887 doi:10.1021/ie50569a035

Morello, V. and Poffenberger, N. (1950). Commercial extraction equipment. *Dow Chemical Company.* 1021-1035.

NIST. (1998). Phosphoric acid. Retrieved March 21, 2021, from https://webbook.nist.gov/cgi/cbook.cgi?ID=C7664382&Mask=2

Perry, R. H., & Green, D. W. (2008). Perry's Chemical Engineers' Handbook. New York: McGraw-Hill.

Peter, S. C. (2018). Reduction of CO2 to Chemicals and Fuels: A Solution to Global Warming and Energy Crisis. *ACS Energy Letters*, *3*(7), 1557-1561. doi:10.1021/acsenergylett.8b00878

Peters, M. S., Timmerhaus, K. D., & West, R. E. (2002). *Plant design and economics for chemical engineers* (5th ed.). McGraw-Hill Professional.

Rodliyah, I., et al. (2015). Extraction of rare earth metals from monazite mineral using acid method. *Indonesian Mining Journal*, *18*(1), 39-45. doi:10.30556/imj.Vol18.No1.2015.305

Salehuddin, A. H., Ismail, A. F., Bahri, C.N., & Aziman, E. S. (2019). Economic analysis of thorium extraction from monazite. *Nuclear Engineering and Technology, 51*(2), 631-640. doi:10.1016/j.net.2018.11.005

Shaeri, M., et al. (2014). Solvent extraction of thorium from nitrate medium by TBP, Cyanex272, and their mixture. *J Radional Nucl Chem.*, *303*, 2093-2099. doi:10.1007/s10967-014-3718-5

Shammas, N.K.; Wang, L.K. Belt Filter Presses. In Biosolids Treatment Processes; Springer: Berlin/Heidelberg, Germany, 2007; pp. 519–539.

Shaw, K. G. (2005). A process for separating thorium compounds from monazite sands (Doctoral dissertation, Iowa State University, 1953). *Ann Arbor, MI: ProQuest Information and Learning Company.*

Tanner Industries, Inc. (2016). *Storage Tanks: Aqua Ammonia*. Tanner Industries, Inc. https://www.tannerind.com/sto-aqua-ammonia.html#:~:text=Storage%20Tanks%3A%20Aqua%20Ammonia&text=Carbon%20steel%20or%20stainless%20steel%20construction%20for%20the%20tank%20is%20recommended.&text=Because%20the%20vapor%20pressure%20of,should%20be%20dry%20and%20cool

Tsinoglou, D., et al. (2004). Transient modelling of flow distribution in automotive catalytic converters. *Applied Mathematical Modelling, 28, 775-794.*

Turton, R., Shaeiwitz, J. A., Bhattacharyya, D., & Whiting, W. B. (2018). Analysis, Synthesis, and Design of Chemical Processes, Fifth Edition (5th ed.). Prentice Hall. https://proquest.safaribooksonline.com/9780134177502

ULINE. (2020). *Bulk Bags - Open Top, Plain Bottom, 35 x 35 x 40".* ULINE Bulk Containers. https://www.uline.com/Product/Detail/S-23459/Bulk-Containers/Bulk-Bags-Open-Top-Plain-Bottom-35-x-35x-40?pricode=WB0746&gadtype=pla&id=S-23459&gclid=Cj0KCQjw3duCBhCAARIsAJeFyPXYPTah1VYqNvZvjg_e__nfnqw0MlW_LAK-CZYHbuZhkmgU9cuw614aAl5REALw_wcB&gclsrc=aw.ds

Union of Concerned Scientists. (2017, Dec. 19). Coal and Air Pollution. Retrieved October 21, 2020, from https://www.ucsusa.org/resources/coal-and-air-pollution#:~:text=Air%20pollution%20from%20coal%2Dfired,environmental%20and%20public%20health%20impacts.

Unnerstall, R. (2020). *Fundamentals of Process Safety*. Personal Collection of Ronald Unnerstall, University of Virginia, Charlottesville VA.

Unnerstall, R. (2021, April 14). Personal interview [Personal Communication].

U.S. Energy Information Administration. (2020). Virginia state energy profile. Retrieved November 6, 2020 from https://www.eia.gov/state/?sid=VA#tabs-4\

Victor, A. C., & Douglas, T. B. (1961). Thermodynamic Properties of Thorium Dioxide from 298 to 1,200 K. *Journal of research of the National Bureau of Standards. Section A, Physics and chemistry*, *65*(2), 105. doi:10.6028/jres.065A.013

Virginia Department of Taxation. (2021). *Corporation Income Tax.* Retrieved April 14, 2020 from https://www.tax.virginia.gov/corporation-income-tax

Wangle T., Tyrpekl V., Cagno S., Delloye T., Larcher O., Cardinaels T., Vleugels J., Verwerft M. (2017). The effect of precipitation and calcination parameters on oxalate derived ThO2 pellets. *Journal of Nuclear Materials*, *495*, 128-137. doi:10.1016/j.jnucmat.2017.07.046

Whatley, M. E. (1953). Purification of thorium by solvent extraction. *Retrospective Theses and Dissertations*. 14049. https://lib.dr.iastate.edu/rtd/14049

White, G. D., Bray, L.A., & Hart, P.E. U.S. Department of Energy. (1980). Optimization of Thorium Oxalate Precipitation Conditions Relative to Thorium Oxide Stability. Pacific Northwest Laboratory.

Wiersma, B, Mickalonis, J, Subramanian, K, & Ketusky, E. (2011). *CORROSION TESTING OF CARBON STEEL IN OXALIC ACID CHEMICAL CLEANING SOLUTIONS*. United States.

World Nuclear Association. (2020). Naturally-Occurring Radioactive Materials (NORM). Retrieved April 07, 2021, from https://www.world-nuclear.org/information-library/safety-and-security/radiation-and-health/naturally-occurring-radioactive-materials-norm.aspx

World Nuclear Association. (2017). Thorium. Retrieved October 08, 2020, from: https://www.world2-nuclear.org/information-library/current-and-future-generation/thoriu.aspx

Zhang, Y. X.; Cai, X.; Zhou, Y.; Zhang, X. X.; Xu, H.; Liu, Z. Q.; Li, X. Y.; Jiang, J. Z. (2007). Structures and Spectroscopic Properties of Bis(phthalocyaninato) Yttrium and Lanthanum Complexes: Theoretical Study Based on Density Functional Theory Calculations J. Phys. Chem. A, *111*, 392– 400. doi:10.1021/jp066157g

XIII. APPENDIX

XIII.A Stream Tables

Table XIII.A.1-1. Overall Mass Balance

Stream	Stream Number	Flow Rate (kg/hr)
98% Sulfuric Acid Feed	1	83.33
Monazite Sand Feed	2	41.67
Leaching Reactor Effluent	3	125.00
Leaching Filter Residue	4	4.17
Filtered Leaching Reactor Effluent	5	120.83
25% Ammonium Hydroxide	6	900.00
Slurry of Ammonium Hydroxide and Sulfates	7	1019.17
Selective Precipitate Effluent	8	1019.17
Rare Earth Waste Stream	9	1013.89
Thorium Hydroxide Precipitate	10	5.28
Concentrate Nitric Acid Feed	11	39.73
Thorium Nitrate Mixture	12	45.01
30% TBP in Kerosene Feed	13	166.68
Aqueous Waste Stream	14	248.52
Organic Phase Thorium	15	841.11
Solvent Recycle Stream	16	833.40
Water Stripping Feed	17	166.68
Extracted Thorium Nitrate	18	174.39
Solid Waste Residue	19	0
Filtered Thorium Nitrate	20	174.39
Oxalic Acid Feed	21	6.38
Thorium Oxalate Slurry	22	180.51
Diluted Nitric Acid Mixture	23	172.51
Solid Thorium Oxalate	24	8.00
Waste Gas	25	3.76
Thorium Oxide	26	4.24

XIII.B Sample Calculations

Leaching Reactor Sample Calculations

Impeller Speed and Power Calculations

Specific power and power number values from empirical data provided by King (2019).

$N_P = 0.75$ $P_S = 1886.8$ (W/m^3) $\rho = 2236$ kg/m^3

$d_i = 0.29$ m $W = 0.037$ m

Power Equation: $P = P_S \pi d_i^2 W / 4 = 4.99$W

Impeller Speed Equation: $N = 60 * \sqrt[3]{\frac{P}{N_p d_i \rho}} = 64\ RPM$

Heat of Reaction Calculation

$$\Delta H_{tot} = \sum_{i=1}^{n} \Delta H_{rxn,i} * n_i$$

The heat of reactions were calculated using yttrium species as an upper bound. The solvated enthalpies for the corresponding phosphates and molar flow rates are as follows:

$\Delta H_{rxn,\ Th} = -1006\ kJ/mol$ $n_{Th} = 0.0052\ kmol/hr$

$\Delta H_{rxn,\ RE} = -754\ kJ/mol$ $n_{RE} = 0.1354\ kmol/hr$

$$\Delta H_{tot} = [(-\ 1006\ \frac{kJ}{mol})(0.0052 \frac{kmol}{hr}) + (-\ 754\ \frac{kJ}{mol})(0.1354 \frac{kmol}{hr})] * 1000\ \frac{mol}{kmol}$$
$$= -107379\ \frac{kJ}{hr}$$

Cooling Water Flow Calculation

$$Q = Cp * m * (T_f - T_i)$$

$Q = -107379\ \frac{kJ}{hr}$ (from above)

$T_i = 30$ ℃, $T_f = 50$ ℃

$Cp = 4.184\ \frac{kJ}{kg*K}$

$$m = \frac{Q}{Cp*(T_f - T_i)} = \frac{-107379\ kJ/hr}{(4.184\ kJ/kg*K)(20°C)} = 1283\ \frac{kg}{hr}$$

Heat Exchanger Cool-Down Calculation

Heat capacity equations for $H_2(SO_4)$, $Y_2(SO_4)_3$, and $Y(PO_4)$ can be found above in equations **III.E.1-(1-3)**, and C_v can be assumed to be equivalent to C_p for aqueous species.

$$\widehat{H}_i = \int_{T_i}^{T_f} C_{p,i}(T)\, dT$$ $T_i = 230^oC$ $T_f = 35^oC$

$$Q = \sum_i m_i C_{p,i}$$ $C_{p,H2O} = 4.184 \frac{kJ}{kg*K}$ $C_{p,H2SO4} = 1.38 \frac{kJ}{kg*K}$

$$Q = -27,889.2\ kJ/hr$$ $T_{C,in} = 30^oC$, $T_{C,out} = 50^oC$

$$Q = mC_{p,H2O}(T_{c,out} - T_{c,in})$$

$$m = 333.28\ kg/hr$$

$$\frac{1}{U} = \frac{1}{U_0} + R_f$$ $U_0 = 850\ W/m^2K$ $R_f = 1.76\times10^{-4}\ m^2K/W$

$$U = 739.39\ \frac{W}{m^2K}$$

$$\Delta T_{lm} = \frac{\Delta T_2 - \Delta T_1}{ln\left(\frac{\Delta T_2}{\Delta T_1}\right)} = \frac{(230-50)-(35-30)}{ln\left(\frac{(230-50)}{(35-30)}\right)} = 48.83K$$

$$S = \frac{T_{tube,out} - T_{tube,in}}{T_{shell,in} - T_{tube,in}} = \frac{50-30}{230-30} = 0.1$$

$$R = \frac{T_{shell,in} - T_{shell,out}}{T_{tube,out} - T_{tube,in}} = \frac{230-35}{50-30} = 9.75$$

Using figure 20.19 from Turton et al. (2018) and assuming 1 shell pass and 2 tube passes, F = 0.5

$$Q = UA_0F\Delta T_{lm}$$

$$A_0 = \frac{27889.2\times1000/3600}{739.39\times0.5\times48.84} = 1.54\ m^2$$

Selective Precipitation Sample Calculations

Heat of Reaction Calculation

$$\Delta H_{tot} = \sum_{i=1}^{n} \Delta H_{rxn,i} * n_i$$

The heat of reactions and mole flows of the reaction (Th, RE, and H_2O) are as follows:

$\Delta H_{rxn,\ Th} = -1934\ kJ/mol$ $n_{Th} = 0.0157\ kmol/hr$

$\Delta H_{rxn,\ RE} = -1940\ kJ/mol$ $n_{RE} = 0.1354\ kmol/hr$

$\Delta H_{rxn,\ H2O} = -682\ kJ/mol$ $n_{H2O} = 0.5983\ kmol/hr$

$$\Delta H_{tot} = [(-1934\ \frac{kJ}{mol})(0.0157\frac{kmol}{hr}) + (-1940\ \frac{kJ}{mol})(0.1354\frac{kmol}{hr}) + (-682\ \frac{kJ}{mol})(0.5983\frac{kmol}{hr})] * 1000\ \frac{mol}{kmol}$$

$$= -700000\ \frac{kJ}{hr}$$

Cooling Water Flow Calculation

$Q = Cp * m * (T_f - T_i)$

Q = -700000 $\frac{kJ}{hr}$ (from above)

T_i = 30 ℃, T_f = 50 ℃

Cp = 4.184 $\frac{kJ}{kg*K}$

$$m = \frac{Q}{Cp*(T_f - T_i)} = \frac{-700000\ kJ/hr}{(4.184\ kJ/kg*K)(20℃)} = 8400\ \frac{kg}{hr}$$

pH Calculation

$pH = -log([H^+])$

$pKa = pH + log(\frac{[AH]}{[A-]})$

$Ka = \frac{[H_3O^+][A^-]}{[HA]}$

$pKa_{H2SO4} = -3$

$Ka_{H2SO4} = 1000$

To calculate the pH of H_2SO_4, where $H_2SO_4 + H_2O \rightarrow H_3O^+ + HSO_4^-$:

$[H_3O^+] = \sqrt{Ka * [H_2SO_4]} = 50.78$

$[H_2SO_4] = 2.579\ \frac{kmol}{m^3}$

$pH = -log([H_3O^+]) = -1.71$

Mixing Pipe Maximum Diameter Calculation

$Re = \frac{\rho dv}{\mu}$

$v = Q / A$

$A = \pi(d/2)^2$

$d = \frac{4\rho Q}{Re\mu\pi}$

$\rho = 1116.43\ kg/m^3$

$\mu = 3.37 * 10^{-3}\ Pa*s$

$Q = 2.74 * 10^{-4}\ m^3/s$

$Re_{turbulent} = 2300$

*d = (4 * 1116.43 * 0.000274) / (2300 * 0.00337 * 3.14)*
= 0.0504 m = 1.98 in

Nitric Acid Reaction Sample Calculations

Specific power and power number values from empirical data provided by King (2019).

$$P_S = 298.28\ (W/m^3)$$

$$d_i = 0.24 m \quad W = 0.0302\ m$$

Power Equation: $P = P_S \pi d_i^2 W / 4 = 0.41\ W$

Impeller Tip Speed = 3 m/s

Impeller Circumference = $d_i \pi$

RPM = $(d_i \pi/3)*60$ = 239

Extraction and Stripping Sample Calculations

Specific power and power number values from empirical data provided by King (2019).

P_S = 969.4 (W/m^3) d_i = 0.79 m W = 0.01 m

Power Equation: $P = (P_S \pi d_i^2 W / 4) * 24$= 114.04W

Oxalate Precipitation Sample Calculations

Heat of Reaction Calculation

$$\Delta H_{tot} = \sum_{i=1}^{n} \Delta H_{rxn,i} * n_i$$

The heat of reactions and mole flows of the reaction (Th, RE, and H_2O) are as follows:

$\Delta H_{rxn,\ Th}$ = -851 *kJ/mol* n_{Th} = 0.0149 *kmol/hr*

$\Delta H_{rxn,\ RE}$ = -851 *kJ/mol* n_{RE} = 0.0019 *kmol/hr*

$\Delta H_{rxn,\ H2O}$ = -109 *kJ/mol* n_{H2O} = 0.0014 *kmol/hr*

$$\Delta H_{tot} = [(-851 \frac{kJ}{mol})(0.0149 \frac{kmol}{hr}) + (-851 \frac{kJ}{mol})(0.0019 \frac{kmol}{hr}) + (-109 \frac{kJ}{mol})(0.0014 \frac{kmol}{hr})] * 1000 \frac{mol}{kmol}$$

$$= -14400 \frac{kJ}{hr}$$

Cooling Water Flow Calculation

$Q = Cp * m * (T_f - T_i)$

Q = -14400 $\frac{kJ}{hr}$(from above)

T_i = 5 ℃, T_f = 20 ℃

Cp = 4.184 $\frac{kJ}{kg*K}$

$$m = \frac{Q}{Cp*(T_f - T_i)} = \frac{-14400\ kJ/hr}{(4.184\ kJ/kg*K)(15°C)} = 360 \frac{kg}{hr}$$

Calcination Sample Calculations

Heat Duty of Kiln Calculation

$$v = \frac{m}{\rho}$$

$m = 8.0\ kg/hr$ $\rho = 4637\ kg/m^3$

$$v = \frac{8\ kg/hr}{4637\ kg/m^3} = 0.00173\ m^3/hr$$

Belt Filter Sample Calculations

Leaching Reactor Belt Filter Calculations - Workable Area

$$\frac{t}{V} = \frac{\alpha_{av}\mu c}{2A^2\Delta p}V$$

Specific resistance of filter cake taken from empirical data provided by Christensen (1983).

$\boldsymbol{\alpha}_{av} = 4.0 * 10^{14}$ m/kg $V = 1.83 * 10^{-4}$ m^3/s

$\mu = 0.0276$ Pa-s $\Delta p = 20265$ Pa

$c = 72.85$ kg/m^3 $t = 60$ s

$A = 0.303$ m^2

XIII.C Calculated Thermodynamic Data

Initially, it was planned to use Aspen Plus with an OLI plug-in to model the process. However, the plug-in could not be obtained and Aspen's standard databank had less than half of the necessary rare earth elements (REEs) and thorium (Th) species. However, in Aspen, new molecular structures can be uploaded and the physical properties can be manually inputted. To test the feasibility of this process, thorium hydroxide was created in the Atomic Simulation Environment (ASE) and optimized using periodic plane-wave calculations. Unfortunately, Aspen could not accurately read the resulting structures' connectivity, and given the lack of thermodynamic data required to model this process, it was determined that Aspen could not be effectively used.

Other computational tools were therefore employed to directly obtain this data, but rigorous computational modeling of thorium is rare and is expensive when pursued. To address these issues, all thermochemical calculations were conducted on yttrium (Y) complexes. It was assumed that the thermochemical data of Y would provide an upper bound for the heat of reaction data of Th and other RE species because the interactions considered in this project are purely ionic, and the ionic radius of Y is generally smaller than the REEs'.

All calculations were performed utilizing Gaussian 16 at the B3LYP level of theory using the default Gaussian convergence criteria (max force < $4.5*10^{-4}$, RMS force < $3*10^{-4}$, max displacement < $1.8*10^{-3}$, RMS displacement < $1.2*10^{-3}$, all criteria in atomic units) (Frish et al. 2016, Becke 1993). All calculations were performed using the LANL2DZ basis and its associated pseudopotentials for Y, and the 6-31G(d,p) basis set for all other atom types, as this functional and basis set choice reproduces Y complex geometries and frequencies well (Zhang et al. 2007). Frequency calculations were performed to obtain thermochemical values for each species in Eqns 1, 2, and 5. Solvation corrections were calculated using the Solvation Model based on Density (SMD) formulation and the parameters for water as implemented by Gaussian 16 (Marenich et al. 2009). After structures were optimized in vacuo, frequency calculations were performed without further optimization regardless of the target species' phase. This was done to avoid oscillations in solvated structure geometry optimizations.

XIII.D Calculated Heat Capacities

Due to the lack of data on rare earth and thorium species heat capacities, they were approximated using yttrium. Using Gaussian 16, optimization and frequency calculations were performed on yttrium sulfate, hydroxide, and nitrate at four different temperatures to obtain the specific heat capacity at these temperatures, as seen in **Figure XIII.D-1**. The lower temperature bound was 25ºC while the upper temperature bound was chosen to be 250ºC, twenty degrees higher than the leaching reactor operating temperature. Polynomial regression was then used to model an equation to determine the heat capacity at a specific temperature or to be integrated across a temperature range. The polynomials are shown in **Table XIII.D-1** and given that all had an r^2 of approximately one, so the equations can be used to accurately model the data in the given temperature range. As yttrium has the same oxidation state as cerium, lanthanum, and neodymium, they were all assumed to follow the same heat capacity trends. While the thorium complexes have slightly different bonding, due to the overall lack of heat capacity data for thorium species and the inability to run specific calculations, the heat capacities for thorium were also assumed to be equivalent to yttrium.

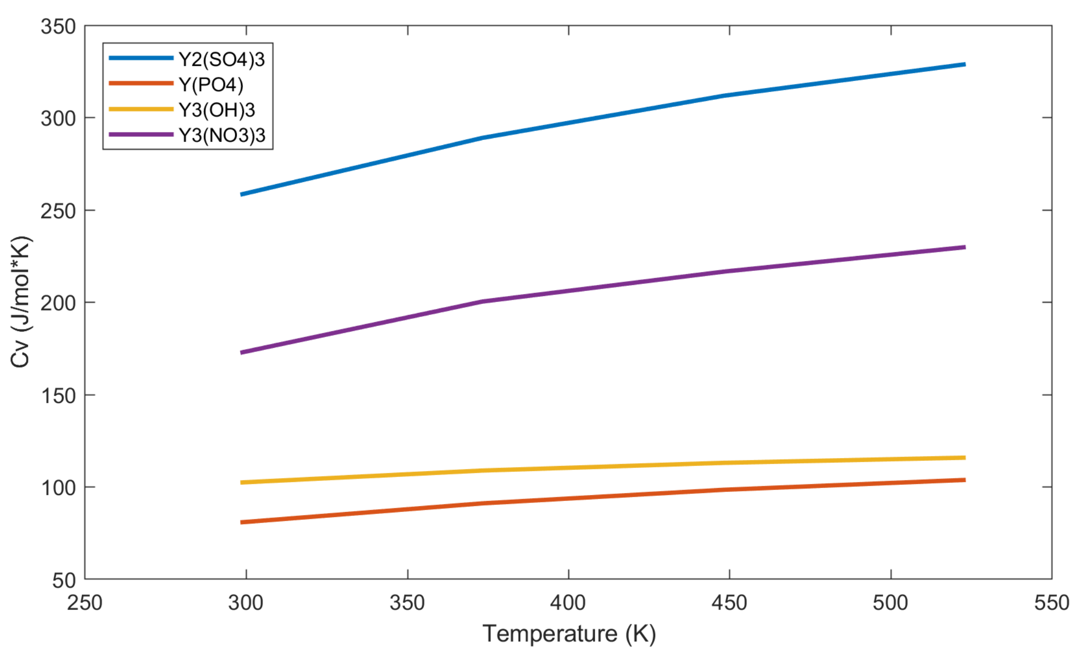

Figure XIII.D-1: Heat Capacities of Yttrium Species at Different Temperatures

Table XIII.D-1: Regressed Heat Capacity Polynomials for Yttrium Species

Species	Heat Capacity Equation (J/mol*K)	r^2
$Y_2(SO_4)_3$	$-6.05471\times10^{-4}T^2 + 8.10281T + 70.5982$	0.999923
$Y(PO_4)$	$-2.19428\times10^{-4}T^2 + 0.28202T - 16.2945$	0.999863
$Y_3(OH)_3$	$-1.62339\times10^{-4}T^2 + 0.19278T + 59.4108$	0.999592
$Y_3(NO_3)_3$	$-6.41547\times10^{-4}T^2 + 0.77735T - 1.65043$	0.998002